estimate the drug metabolism capacity, the amount of metabolites must be measured during the time when production of metabolites is linearly detected (generally before 24 h). To the best of our knowledge, there have been few reports that have examined various drugs metabolism capacity of hESC-hepa and hiPSC-hepa in detail.

In the present study, seven candidate genes (*FOXA2*, *HEX*, *HNF1α*, *HNF1β*, *HNF4α*, *HNF6*, and *SOX17*) were transduced into each stage of hepatic differentiation from hESCs by using an adenovirus (Ad) vector to screen for hepatic differentiation-promoting factors. Then, hepatocyte-related gene expression profiles and hepatocyte functions in hESC-hepa and hiPSC-hepa generated by the optimized protocol, were examined to investigate whether these cells have PHs characteristics. We used nine drugs, which are metabolized by various CYP enzymes and UDP-glucuronosyltransferases (UGTs), to determine whether the hESC-hepa and hiPSC-hepa have drug metabolism capacity. Furthermore, hESC-hepa and hiPSC-hepa were examined to determine whether these cells may be applied to evaluate drug-induced cytotoxicity.

Materials and methods

In vitro differentiation

Before the initiation of cellular differentiation, the medium of hESCs and hiPSCs was exchanged for a defined serum-free medium, hESF9, and cultured as previously reported [9]. The differentiation protocol for the induction of DE cells, hepatoblasts, and hepatocytes was based on our previous report with some modifications [5,6]. Briefly, in mesendoderm differentiation, hESCs and hiPSCs were dissociated into single cells by using Accutase (Millipore) and cultured for 2 days on Matrigel (BD biosciences) in differentiation hESF-DIF medium which contains 100 ng/ml Activin A (R&D Systems) and 10 ng/ml bFGF (hESF-DIF medium, Cell Science & Technology Institute; differentiation hESF-DIF medium was supplemented with 10 μg/ml human recombinant insulin, 5 μg/ml human apotransferrin, 10 μM 2-mercaptoethanol, 10 μM ethanolamine, 10 μM sodium selenite, and 0.5 mg/ml bovine serum albumin, all from Sigma). To generate DE cells, mesendoderm cells were transduced with 3000 VP/cell of Ad-FOXA2 for 1.5 h on day 2 and cultured until day 6 on Matrigel in differentiation hESF-DIF medium supplemented with 100 ng/ml Activin A and 10 ng/ml bFGF. For induction of hepatoblasts, the DE cells were transduced with each 1500 VP/cell of Ad-FOXA2 and Ad-HNF1α for 1.5 h on day 6 and cultured for 3 days on Matrigel in hepatocyte culture medium (HCM, Lonza) supplemented with 30 ng/ml bone morphogenetic protein 4 (BMP4, R&D Systems) and 20 ng/ml FGF4 (R&D Systems). In hepatic expansion, the hepatoblasts were transduced with each 1500 VP/cell of Ad-FOXA2 and Ad-HNF1α for 1.5 h on day 9 and cultured for 3 days on Matrigel in HCM supplemented with 10 ng/ml hepatocyte growth factor (HGF), 10 ng/ml FGF1, 10 ng/ml FGF4, and 10 ng/ml FGF10 (all from R&D Systems). In hepatic maturation, cells were cultured for 8 days on Matrigel in L15 medium (Invitrogen) supplemented with 8.3% tryptose phosphate broth (BD biosciences), 10% FBS (Vita), 10 μM hydrocortisone 21-hemisuccinate (Sigma), 1 μM insulin, 25 mM $NaHCO_3$ (Wako), 20 ng/ml HGF, 20 ng/ml Oncostatin M (OsM, R&D systems), and 10^{-6} M Dexamethasone (DEX, Sigma).

Results

Recently, we showed that the sequential transduction of SOX17, HEX, and HNF4α into hESC-derived mesendoderm, DE, and hepatoblasts, respectively, leads to efficient generation of the hESC-hepa [5–7]. In the present study, to further improve the differentiation efficiency towards hepatocytes, we screened for hepatic differentiation-promoting transcription factors. Seven candidate genes involved in liver development were selected. We then examined the function of the hESC-hepa and hiPSC-hepa generated by the optimized protocol for pharmaceutical use in detail.

Efficient hepatic differentiation by Ad-FOXA2 and Ad-HNF1α transduction

To perform efficient DE differentiation, T-positive hESC-derived mesendoderm cells (day 2) (Supplementary Fig. 1) were transduced with Ad vector expressing various transcription factors (Ad-FOXA2, Ad-HEX, Ad-HNF1α, Ad-HNF1β, Ad-HNF4α, Ad-HNF6, and Ad-SOX17 were used in this study). We ascertained the expression of *FOXA2*, *HEX*, *HNF1α*, *HNF1β*, *HNF4α*, *HNF6*, or *SOX17* in Ad-FOXA2-, Ad-HEX-, Ad-HNF1α-, Ad-HNF1β-, Ad-HNF4α-, Ad-HNF6-, or Ad-SOX17-transduced cells, respectively (Supplementary Fig. 2). We also verified that there was no cytotoxicity of the cells transduced with Ad vector until the total amount of Ad vector reached 12,000 VP/cell (Supplementary Fig. 3). Each transcription factor was expressed in hESC-derived mesendoderm cells on day 2 by using Ad vector, and the efficiency of DE differentiation was examined (Fig. 1A). The DE differentiation efficiency based on CXCR4-positive cells was the highest when Ad-SOX17 or Ad-FOXA2 were transduced (Fig. 1B). To investigate the difference between Ad-FOXA2-transduced cells and Ad-SOX17-transduced cells, gene expression levels of markers of undifferentiated cells, mesendoderm cells, DE cells, and extraembryonic endoderm cells were examined (Fig. 1C). The expression levels of extraembryonic endoderm markers of Ad-SOX17-transduced cells were higher than those of Ad-FOXA2-transduced cells. Therefore, we concluded that FOXA2 transduction is suitable for use in selective DE differentiation.

To promote hepatic commitment, various transcription factors were transduced into DE cells and the resulting phenotypes were examined on day 9 (Fig. 1D). Nearly 100% of the population of Ad-FOXA2-transduced cells and Ad-HNF1α-transduced cells was α-fetoprotein (AFP)-positive (Fig. 1E). We expected that hepatic commitment would be further accelerated by combining FOXA2 and HNF1α transduction. The DE cells were transduced with both Ad-FOXA2 and Ad-HNF1α, and then the gene expression levels of *CYP3A7* [10], which is a marker of fetal hepatocytes, were evaluated (Fig. 1F). When both Ad-FOXA2 and Ad-HNF1α were transduced into DE cells, the promotion of hepatic commitment was greater than in Ad-FOXA2-transduced cells or Ad-HNF1α-transduced cells.

To promote hepatic expansion and maturation, we transduced various transcription factors into hepatoblasts on day 9 and 12 and the resulting phenotypes were examined on day 20 (Fig. 1G). We ascertained that the hepatoblast population was efficiently expanded by addition of HGF, FGF1, FGF4, and FGF10 (Supplementary Fig. 4). The hepatic differentiation efficiency based on asialoglycoprotein receptor 1 (ASGR1)-positive cells was measured on day 20, demonstrating that FOXA2, HNF1α, and HNF4α transduction could promote efficient hepatic maturation (Fig. 1H). To investigate the phenotypic difference between Ad-FOXA2-, Ad-HNF1α-, and Ad-HNF4α-transduced cells, gene expression levels of early hepatic markers, mature hepatic markers, and biliary markers were examined (Fig. 1I). Gene expression levels of mature hepatic markers were up-regulated by FOXA2, HNF1α, or HNF4α transduction. FOXA2 transduction strongly upregulated gene expression levels of both early hepatic markers and mature hepatic markers, while HNF1α or HNF4α transduc-

Molecular and Cell Biology

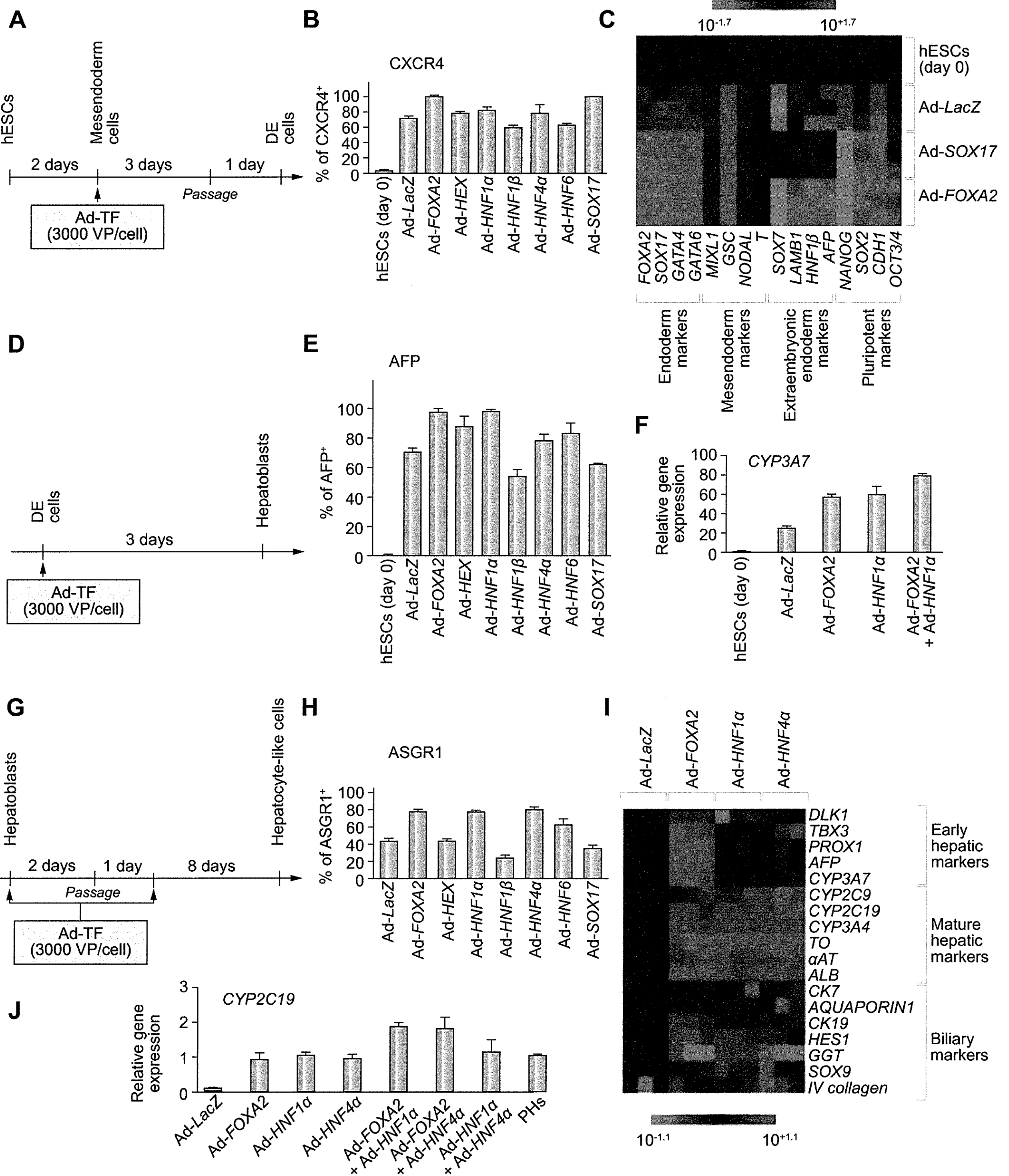

Fig. 1. Efficient hepatic differentiation from hESCs by FOXA2 and HNF1α transduction. (A) The schematic protocol describes the strategy for DE differentiation from hESCs (H9). Mesendoderm cells (day 2) were transduced with 3000 VP/cell of transcription factor (TF)-expressing Ad vector (Ad-TF) for 1.5 h and cultured as described in Fig. 2A. (B) On day 5, the efficiency of DE differentiation was measured by estimating the percentage of CXCR4-positive cells using FACS analysis. (C) The gene expression profiles were examined on day 5. (D) Schematic protocol describing the strategy for hepatoblast differentiation from DE. DE cells (day 6) were transduced with 3000 VP/cell of Ad-TF for 1.5 h and cultured as described in Fig. 2A. (E) On day 9, the efficiency of hepatoblast differentiation was measured by estimating the percentage of AFP-positive

Molecular and Cell Biology

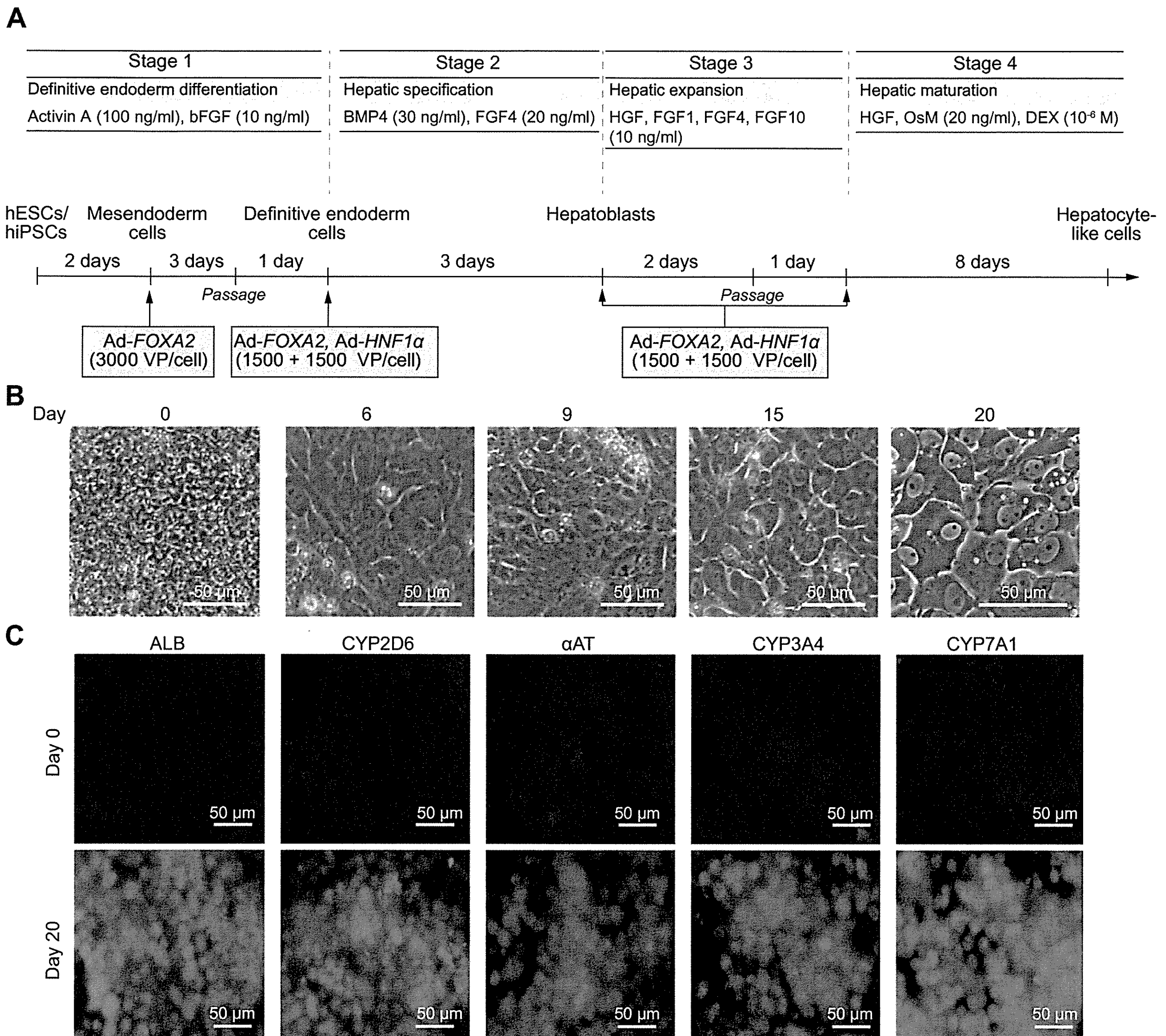

Fig. 2. Hepatic differentiation of hESCs and hiPSCs by FOXA2 and HNF1α transduction. (A) The differentiation procedure of hESCs and hiPSCs into hepatocytes via DE cells and hepatoblasts is schematically shown. Details of the hepatic differentiation procedure are described in Materials and methods. (B) Sequential morphological changes (day 0–20) of hESCs (H9) differentiated into hepatocytes are shown. (C) The expression of the hepatocyte markers (ALB, CYP2D6, αAT, CYP3A4, and CYP7A1, all green) was examined by immunohistochemistry on day 0 and 20. Nuclei were counterstained with DAPI (blue).

tion did not up-regulate the gene expression levels of early hepatic markers. Next, multiple transduction of transcription factors was performed to promote further hepatic maturation. The combination of Ad-FOXA2 and Ad-HNF1α transduction and the combination of Ad-FOXA2 and Ad-HNF4α transduction result in the most efficient hepatic maturation, judged from the gene expression levels of *CYP2C19* (Fig. 1J). This may happen because the mixture of immature hepatocytes and mature hepatocytes coor-

cells using FACS analysis. (F) The gene expression level of *CYP3A7* was measured by real-time RT-PCR on day 9. On the *y* axis, the gene expression level of *CYP3A7* in hESCs (day 0) was taken as 1.0. (G) The schematic protocol describes the strategy for hepatic differentiation from hepatoblasts. Hepatoblasts (day 9) were transduced with 3000 VP/cell of Ad-TF for 1.5 h and cultured as described in Fig. 2A. (H) On day 20, the efficiency of hepatic differentiation was measured by estimating the percentage of ASGR1-positive cells using FACS analysis. The detail results of FACS analysis are shown in Supplementary Table 1. (I) Gene expression profiles were examined on day 20. (J) Hepatoblasts (day 9) were transduced with 3000 VP/cell of Ad-TFs (in the case of combination transduction of two types of Ad vector, 1500 VP/cell of each Ad-TF was transduced) for 1.5 h and cultured. Gene expression levels of *CYP2C19* were measured by real-time RT-PCR on day 20. On the *y* axis, the gene expression level of *CYP2C19* in PHs, which were cultured for 48 h after the cells were plated, was taken as 1.0. All data are represented as mean ± SD (n = 3).

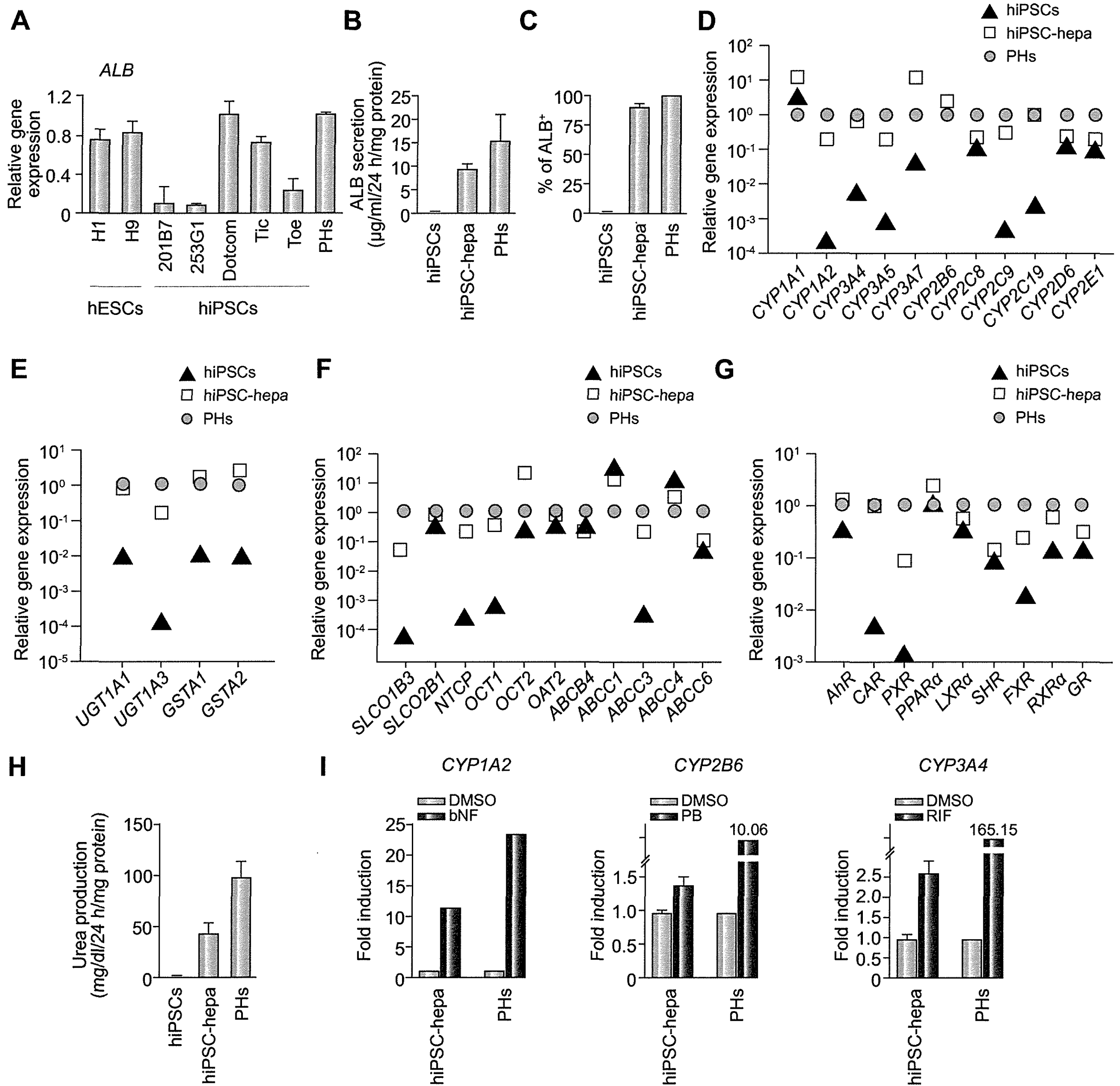

Fig. 3. The hepatic characterization of hiPSC-hepa. hESCs (H1 and H9) and hiPSCs (201B7, 253G1, Dotcom, Tic, and Toe) were differentiated into hepatocyte-like cells as described in Fig. 2A. (A) On day 20, the gene expression level of *ALB* was examined by real-time RT-PCR. On the *y* axis, the gene expression level of *ALB* in PHs, which were cultured for 48 h after cells were plated, was taken as 1.0. (B–I) hiPSCs (Dotcom) were differentiated into hepatocyte-like cells as described in Fig. 2A. (B) The amount of ALB secretion was examined by ELISA in hiPSCs, hiPSC-hepa, and PHs. (C) hiPSCs, hiPSC-hepa, and PHs were subjected to immunostaining with anti-ALB antibodies, and then the percentage of ALB-positive cells was examined by flow cytometry. (D–G) The gene expression levels of CYP enzymes (D), conjugating enzymes (E), hepatic transporters (F), and hepatic nuclear receptors (G) were examined by real-time RT-PCR in hiPSCs, hiPSC-hepa, and PHs. On the *y* axis, the expression level of PHs is indicated. (H) The amount of urea secretion was examined in hiPSCs, hiPSC-hepa, and PHs. (I) Induction of *CYP1A2*, *2B6*, or *3A4* by DMSO or inducer (bNF, PB, or RIF) of hiPSC-hepa and PHs, cultured for 48 h after the cells were plated, was examined. On the y axis, the gene expression levels of *CYP1A2*, *2B6*, or *3A4* in DMSO-treated cells, which were cultured for 48 h, were taken as 1.0. All data are represented as mean ± SD (n = 3).

dinately works to induce hepatocyte functions. Taken together, efficient hepatic differentiation could be promoted by using the combination of FOXA2 and HNF1α transduction at the optimal stage of differentiation (Fig. 2A). At the stage of hepatic expansion and maturation, Ad-HNF4α can be substituted for Ad-HNF1α (Fig. 1J). Interestingly, cell growth was delayed by FOXA2 and HNF4α transduction (Supplementary Fig. 5). This delay in cell proliferation might be due to promoted maturation by FOXA2 and HNF1α transduction. As the hepatic differentiation proceeds, the morphology of hESCs gradually changed into a typical hepatocyte morphology, with distinct round nuclei and a polygonal shape (Fig. 2B), and the expression levels of hepatic markers

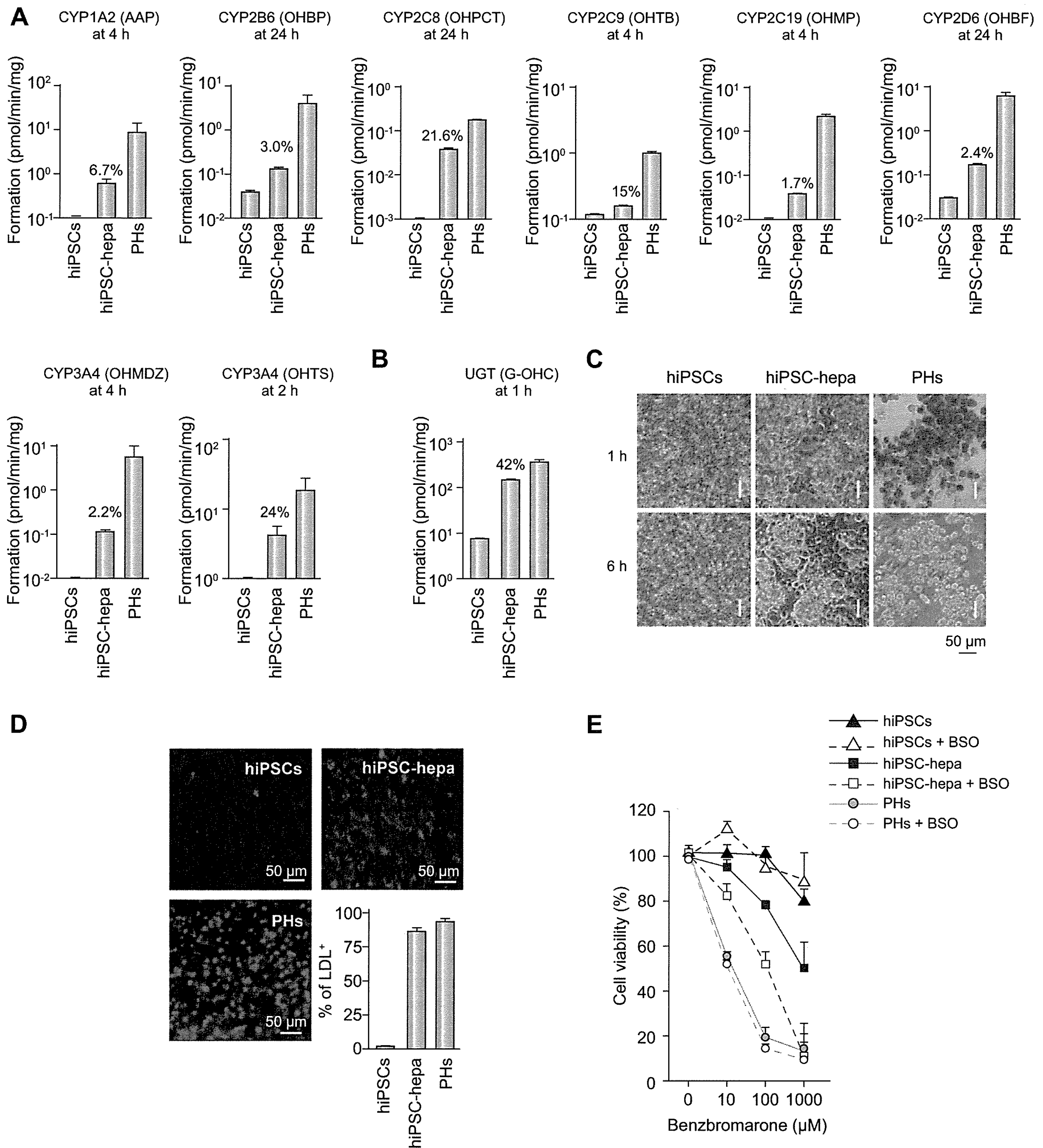

Fig. 4. Evaluation of the drug metabolism capacity and hepatic transporter activity of hiPSC-hepa. hiPSCs (Dotcom) were differentiated into hepatocytes as described in Fig. 2A. (A and B) Quantitation of metabolites in hiPSCs, hiPSC-hepa, and PHs, which were cultured for 48 h after the cells were plated, was examined by treating nine substrates (Phenacetin, Bupropion, Paclitazel, Tolbtamide, *S*-mephenytoin, Bufuralol, Midazolam, Testosterone, and Hydroxyl coumarin; these compounds are substrates for CYP1A2, 2B6, 2C8, 2C19, 2D6, 3A4, 3A4 (A) and UGT (B), respectively), and then supernatants were collected at the indicated time. The quantity of metabolites (Acetaminophen [AAP], Hydroxybupropion [OHBP], 6α-hydroxypaclitaxel [OHPCT], Hydroxytolbutamide [OHTB], 4′-hydroxymephenytoin [OHMP], 1′-hydroxybufuralol [OHBF], 1′-hydroxymidazolam [OHMDZ], 6β-hydroxytestosterone [OHTS], 7-Hydroxycoumarin glucuronide [G-OHC], respectively) was measured by LC-MS/MS. The ratios of the activity levels in hiPSC-hepa to the activity levels in PHs rate are indicated in the graph. (C) hiPSCs, hiPSC-hepa, and PHs were examined for their ability to take up ICG (top) and release it 6 h thereafter (bottom). (D) hiPSCs, hiPSC-hepa, and PHs were cultured with medium containing Alexa-Flour 488-labeled LDL (green) for 1 h, and immunohistochemistry was performed. Nuclei were counterstained with DAPI (blue). The percentage of LDL-positive cells was also measured by FACS analysis. (E)

(ALB, CYP2D6, alpha-1-antitrypsin [αAT], CYP3A4, and CYP7A1) increased (Fig. 2C). Hepatic gene expression levels (Supplementary Fig. 6A), amount of ALB secretion (Supplementary Fig. 6B), and CYP2C9 activity level (Supplementary Fig. 6C) of Ad-FOXA2- and Ad-HNF1α-transduced cells were significantly higher than those of Ad-SOX17-, Ad-HEX-, and Ad-HNF4α-transduced cells. These results indicated that FOXA2 and HNF1α transduction promotes more efficiently hepatic differentiation than SOX17, HEX, and HNF4α transduction.

Characterization of the hESC-hepa/hiPSC-hepa

As we have previously reported [6], hepatic differentiation efficiency differs among hESC/hiPSC lines. Therefore, it is necessary to select a hESC/hiPSC line that is suitable for hepatic maturation in the case of medical applications such as drug screening. In the present study, two hESC lines and five hiPSCs lines were differentiated into hepatocyte-like cells, and then their gene expression levels of *ALB* (Fig. 3A) and *CYP3A4* (Supplementary Fig. 7A), and their CYP3A4 activities (Supplementary Fig. 7B) were compared. These data suggest that the iPSC line, Dotcom [11,12], was the most suitable for hepatocyte maturation. To examine whether the iPSC (Dotcom)-hepa has enough hepatic functions as compared with PHs, the amount of albumin (ALB) secretion (Fig. 3B) and the percentage of ALB-positive cells (Fig. 3C) were measured on day 20. The amount of ALB secretion in hiPSC-hepa was similar to that in PHs and the percentage of ALB-positive cells was approximately 90% in iPSC-hepa. We also confirmed that the gene expression levels of CYP enzymes (Fig. 3D), conjugating enzymes (Fig. 3E), hepatic transporters (Fig. 3F), and hepatic nuclear receptors (Fig. 3G) in hiPSC-hepa were similar to those of PHs, although some of them were still lower than those of PHs. Because the gene expression level of the fetal CYP isoform, *CYP3A7*, in hiPSC-hepa was higher than that of PHs, mature hepatocytes and hepatic precursors were still mixed. We have previously confirmed that Ad vector-mediated gene expression in the hepatoblasts (day 9) continued until day 14 and almost disappeared on day 18 [7]. Therefore, the hepatocyte-related genes expressed in hiPSC-hepa are not directly regulated by exogenous FOXA2 or HNF1α. Taken together, endogenous hepatocyte-related genes in hiPSC-hepa should have been upregulated by FOXA2 and HNF1α transduction.

To further confirm that hiPSC-hepa have sufficient levels of hepatocyte functions, we evaluated the ability of urea secretion (Fig. 3H) and glycogen storage (Supplementary Fig. 8). The amount of urea secretion in hiPSC-hepa was about half of that in PHs. HiPSC-hepa exhibited abundant storage of glycogen. Because CYP1A2, 2B6, and 3A4 are involved in the metabolism of a significant proportion of the currently available commercial drugs, we tested the induction of *CYP1A2*, *2B6*, and *3A4* by chemical stimulation (Fig. 3I). *CYP1A2*, *2B6*, and *3A4* are induced by β-naphthoflavone [bNF], phenobarbital [PB], or rifampicin [RIF], respectively. Although undifferentiated hiPSCs did not respond to either bNF, PB, or RIF (data not shown), hiPSC-hepa produced more metabolites in response to chemical stimulation, suggesting that inducible CYP enzymes were detectable in hiPSC-hepa (Fig. 3I). However, the induction potency of *CYP1A2*, *2B6*, and *3A4* in hiPSC-hepa were lower than that in PHs.

Drug metabolism capacity and hepatic transporter activity of hiPSC-hepa

Because metabolism and detoxification in the liver are mainly executed by CYP enzymes, conjugating enzymes, and hepatic transporters, it is important to assess the function of these enzymes and transporters in hiPSC-hepa. Among the various enzymes in liver, CYP1A2, 2B6, 2C8, 2C9, 2C19, 2D6 and 3A4, UGT are the important phase I and II enzymes responsible for metabolism. Nine substrates, Phenacetin, Bupropion, Paclitazel, Tolbtamide, *S*-mephenytoin, Bufuralol, Midazolam, Testosterone, and Hydroxyl coumarin, which are the substrates of CYP1A2, 2B6, 2C8, 2C9, 2C19, 2D6, 3A4, 3A4 (Fig. 4A), and UGT (Fig. 4B), respectively, were used to estimate the drug metabolism capacity of hiPSC-hepa compared with that of PHs. To precisely estimate the drug metabolism capacity, the amounts of metabolites were measured during the phase when production of metabolites was linear (Supplementary Fig. 9). These results indicated that our hiPSC-hepa have the capacity to metabolize these nine substrates, although the activity levels were lower than those of PHs. The hepatic functions of hiPSC-hepa were further evaluated by examining the ability to uptake Indocyanine Green (ICG) and LDL (Fig. 4C and D, respectively). In addition to PHs, hiPSC-hepa had the ability to uptake ICG and to excrete ICG in a culture without ICG for 6 h (Fig. 4C), and to uptake LDL (Fig. 4D). These results suggest that hiPSC-hepa have enough CYP enzyme activity, conjugating enzyme activity, and hepatic transporter activity to metabolize various drugs.

To examine whether our hiPSC-hepa could be used to predict metabolism-mediated toxicity, hiPSC-hepa were incubated with Benzbromarone, which is known to generate toxic metabolites, and then cell viability was measured (Fig. 4E). Cell viability of hiPSC-hepa was decreased depending on the concentration of Benzbromarone. However, cell viability of hiPSC-hepa was much higher than that of PHs. To detect drug-induced cytotoxicity with high sensitivity in hiPSC-hepa, these cells were treated with Buthionine-SR-sulfoximine (BSO), which depletes cellular GST, and result in a decrease of cell viability of hiPSC-hepa as compared with that of non-treated cells (Fig. 4E). These results indicated that hiPSC-hepa would be more useful in drug screening under a condition of knockdown of conjugating enzyme activity.

Discussion

The establishment of an efficient hepatic differentiation technology from hESCs and hiPSCs would be important for the application of hESC-hepa and hiPSC-hepa to drug toxicity screening. Although we have previously reported that sequential transduc-

The cell viability of hiPSCs, hiPSC-hepa, PHs, and their BSO-treated cells (0.4 mM BSO was pre-treated for 24 h) was assessed by Alamar Blue assay after 48-hr exposure to differe2nt concentrations of benzbromarone. The cell viability is expressed as a percentage of that in cells treated only with solvent. All data are represented as mean ± SD (n = 3).

tion of SOX17, HEX, and HNF4α into hESC-derived cells could promote efficient hepatic differentiation [7], further hepatic maturation of the hESC-hepa and hiPSC-hepa was needed for this application. To further improve the differentiation efficiency of every step of hepatic differentiation (hESC to DE cells, DE cells to hepatoblasts, and hepatoblasts to hESC-hepa), we initially performed a screening of transcription factors. In the stage of DE differentiation, FOXA2 transduction could promote the most efficient DE differentiation (Fig. 1C). In the stage of hepatic commitment, expansion, and maturation, the combination of FOXA2 and HNF1α transduction strongly promoted hepatic commitment and maturation (Fig. 1F and J), although in the stage of hepatic expansion and maturation, HNF4α transduction was as efficient as that of HNF1α (Fig. 1J). Since HNF1α is one of the target genes of HNF4α [13], the signaling through HNF4α to HNF1α would be important for efficient hepatic expansion and maturation. Considering these results together, we ascertained a pair of two transcription factors, FOXA2 and HNF1α, that could promote efficient hepatic differentiation from hESCs. In embryogenesis, the expression of FOXA2 and HNF1α is initially detected in DE or hepatoblasts, respectively and the expression levels of both FOXA2 and HNF1α are elevated as the liver develops [14,15]. Therefore, our hepatic differentiation technology, which employs FOXA2 and HNF1α transduction, might mimic the gene expression pattern during embryogenesis.

We found that the gene expression levels of CYP enzymes, conjugating enzymes, hepatic transporters, and hepatic nuclear receptors were upregulated by FOXA2 and HNF1α transduction (Fig. 3D–G). In contrast to the high expression levels of hepatocyte-related genes, CYP induction potency and the drug metabolism capacity of our hiPSC-hepa were lower than those of PHs (Figs. 3I and 4A and B). One of the possible reasons for the difference between gene expression levels of CYP enzymes and CYP induction activity might be that there were insufficient expression levels of hepatic nuclear receptors (such as *PXR*, *SHR*, and *FXR*) in hiPSC-hepa (Fig. 3G). Because many CYPs require high expression levels of hepatic nuclear receptor for efficient drug metabolism [16], transduction of these hepatic nuclear receptor genes in hiPSC-hepa or development of a differentiation method that induces high expression of these nuclear receptors might improve the drug metabolic capacity. Another explanation for the low CYP activities in hiPSC-hepa, maybe that hiPSCs were established from an individual with low CYP activities; infact, it is known that large individual differences in CYP activities are observed among individuals. It might be important to use a hiPSC line established from a person with high CYP activities. It is essential to investigate the reasons behind this significant discordance, an issue that our group is currently planning to study.

In summary, our method, consisting of sequential FOXA2 and HNF1α transduction along with the addition of adequate soluble factors at each step of differentiation, is a valuable tool for the efficient generation of functional hepatocytes derived from hESCs and hiPSCs. The hiPSC-hepa exhibited a number of hepatocyte functions (such as ALB secretion, uptake of LDL or ICG, glycogen storage, and drug metabolism capacity). In addition, the hiPSC-hepa were successfully applied to the evaluation of drug-induced cytotoxicity. Therefore, the hESC-hepa and hiPSC-hepa might be used for drug screening in early phases of pharmaceutical development.

Conflict of interest

The authors who have taken part in this study declared that they do not have anything to disclose regarding funding or conflict of interest with respect to this manuscript.

Acknowledgements

We thank Misae Nishijima, Nobue Hirata, Miki Yoshioka, and Hiroko Matsumura for their excellent technical support. We thank Ms. Ong Tyng Tyng for critical reading of the manuscript. HM, MKF, and TH were supported by grants from the Ministry of Health, Labor, and Welfare of Japan. HM was also supported by Japan Research foundation For Clinical Pharmacology, The Nakatomi Foundation, and The Uehara Memorial Foundation. K. Kawabata was supported by Grants from the Ministry of Education, Sports, Science and Technology of Japan (20200076) and the Ministry of Health, Labor, and Welfare of Japan. K. Katayama and FS were supported by Program for Promotion of Fundamental Studies in Health Sciences of the National Institute of Biomedical Innovation (NIBIO).

Supplementary data

Supplementary data associated with this article can be found, in the online version, at http://dx.doi.org/10.1016/j.jhep.2012.04.038.

References

[1] Thomson JA, Itskovitz-Eldor J, Shapiro SS, Waknitz MA, Swiergiel JJ, Marshall VS, et al. Embryonic stem cell lines derived from human blastocysts. Science 1998;282:1145–1147.
[2] Takahashi K, Tanabe K, Ohnuki M, Narita M, Ichisaka T, Tomoda K, et al. Induction of pluripotent stem cells from adult human fibroblasts by defined factors. Cell 2007;131:861–872.
[3] Clayton DF, Darnell Jr JE. Changes in liver-specific compared to common gene transcription during primary culture of mouse hepatocytes. Mol Cell Biol 1983;3:1552–1561.
[4] Snykers S, De Kock J, Rogiers V, Vanhaecke T. In vitro differentiation of embryonic and adult stem cells into hepatocytes: state of the art. Stem cells 2009;27:577–605.
[5] Inamura M, Kawabata K, Takayama K, Tashiro K, Sakurai F, Katayama K, et al. Efficient generation of hepatoblasts from human ES cells and iPS cells by transient overexpression of homeobox gene HEX. Mol Ther 2011;19:400–407.
[6] Takayama K, Inamura M, Kawabata K, Tashiro K, Katayama K, Sakurai F, et al. Efficient and directive generation of two distinct endoderm lineages from human ESCs and iPSCs by differentiation stage-specific SOX17 transduction. PLoS One 2011;6:e21780.
[7] Takayama K, Inamura M, Kawabata K, Katayama K, Higuchi M, Tashiro K, et al. efficient generation of functional hepatocytes from human embryonic stem cells and induced pluripotent stem cells by HNF4alpha transduction. Mol Ther 2012;20:127–137.
[8] Duan Y, Ma X, Zou W, Wang C, Bahbahan IS, Ahuja TP, et al. Differentiation and characterization of metabolically functioning hepatocytes from human embryonic stem cells. Stem cells 2010;28:674–686.
[9] Furue MK, Na J, Jackson JP, Okamoto T, Jones M, Baker D, et al. Heparin promotes the growth of human embryonic stem cells in a defined serum-free medium. Proc Natl Acad Sci U S A 2008;105:13409–13414.
[10] Lacroix D, Sonnier M, Moncion A, Cheron G, Cresteil T. Expression of CYP3A in the human liver–evidence that the shift between CYP3A7 and CYP3A4 occurs immediately after birth. Eur J Biochem 1997;247:625–634.

[11] Nagata S, Toyoda M, Yamaguchi S, Hirano K, Makino H, Nishino K, et al. Efficient reprogramming of human and mouse primary extra-embryonic cells to pluripotent stem cells. Genes Cells 2009;14:1395–1404.
[12] Makino H, Toyoda M, Matsumoto K, Saito H, Nishino K, Fukawatase Y, et al. Mesenchymal to embryonic incomplete transition of human cells by chimeric OCT4/3 (POU5F1) with physiological co-activator EWS. Exp Cell Res 2009;315:2727–2740.
[13] Gragnoli C, Lindner T, Cockburn BN, Kaisaki PJ, Gragnoli F, Marozzi G, et al. Maturity-onset diabetes of the young due to a mutation in the hepatocyte nuclear factor-4 alpha binding site in the promoter of the hepatocyte nuclear factor-1 alpha gene. Diabetes 1997;46:1648–1651.
[14] Ang SL, Wierda A, Wong D, Stevens KA, Cascio S, Rossant J, et al. The formation and maintenance of the definitive endoderm lineage in the mouse: involvement of HNF3/forkhead proteins. Development 1993;119: 1301–1315.
[15] Kyrmizi I, Hatzis P, Katrakili N, Tronche F, Gonzalez FJ, Talianidis I. Plasticity and expanding complexity of the hepatic transcription factor network during liver development. Genes Dev 2006;20:2293–2305.
[16] Lehmann JM, McKee DD, Watson MA, Willson TM, Moore JT, Kliewer SA. The human orphan nuclear receptor PXR is activated by compounds that regulate CYP3A4 gene expression and cause drug interactions. J Clin Invest 1998;102:1016–1023.

Biomaterials 34 (2013) 1781–1789

Contents lists available at SciVerse ScienceDirect

Biomaterials

journal homepage: www.elsevier.com/locate/biomaterials

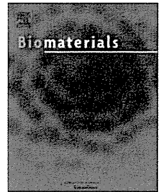

3D spheroid culture of hESC/hiPSC-derived hepatocyte-like cells for drug toxicity testing

Kazuo Takayama [a,b], Kenji Kawabata [b,c], Yasuhito Nagamoto [a,b], Keisuke Kishimoto [a,b], Katsuhisa Tashiro [b], Fuminori Sakurai [a], Masashi Tachibana [a], Katsuhiro Kanda [d], Takao Hayakawa [e], Miho Kusuda Furue [f,g], Hiroyuki Mizuguchi [a,b,h,*]

[a] *Laboratory of Biochemistry and Molecular Biology, Graduate School of Pharmaceutical Sciences, Osaka University, Osaka 565-0871, Japan*
[b] *Laboratory of Stem Cell Regulation, National Institute of Biomedical Innovation, Osaka 567-0085, Japan*
[c] *Laboratory of Biomedical Innovation, Graduate School of Pharmaceutical Sciences, Osaka University, Osaka 565-0871, Japan*
[d] *Pharma Business Project, Corporate Projects Center, Corporate Strategy Division, Hitachi High-Technologies Corporation, Ibaraki 312-8504, Japan*
[e] *Pharmaceutical Research and Technology Institute, Kinki University, Osaka 577-8502, Japan*
[f] *Laboratory of Embryonic Stem Cell Cultures, Department of Disease Bioresources Research, National Institute of Biomedical Innovation, Osaka 567-0085, Japan*
[g] *Department of Embryonic Stem Cell Research, Field of Stem Cell Reseach, Institute for Frontier Medical Sciences, Kyoto University, Kyoto 606-8507, Japan*
[h] *The Center for Advanced Medical Engineering and Informatics, Osaka University, Osaka 565-0871, Japan*

A R T I C L E I N F O

Article history:
Received 11 September 2012
Accepted 20 November 2012
Available online 8 December 2012

Keywords:
Hepatocyte-like cell
Human ES cell
Human iPS cell
Nanopillar plate
Drug screening

A B S T R A C T

Although it is expected that hepatocyte-like cells differentiated from human embryonic stem (ES) cells or induced pluripotent stem (iPS) cells will be utilized in drug toxicity testing, the actual applicability of hepatocyte-like cells in this context has not been well examined so far. To generate mature hepatocyte-like cells that would be applicable for drug toxicity testing, we established a hepatocyte differentiation method that employs not only stage-specific transient overexpression of hepatocyte-related transcription factors but also a three-dimensional spheroid culture system using a Nanopillar Plate. We succeeded in establishing protocol that could generate more matured hepatocyte-like cells than our previous protocol. In addition, our hepatocyte-like cells could sensitively predict drug-induced hepatotoxicity, including reactive metabolite-mediated toxicity. In conclusion, our hepatocyte-like cells differentiated from human ES cells or iPS cells have potential to be applied in drug toxicity testing.

© 2012 Elsevier Ltd. All rights reserved.

1. Introduction

Hepatocyte-like cells that are generated from human embryonic stem cells (hESCs) [1] or human induced pluripotent stem cells (hiPSCs) [2] are expected to be used in drug screening instead of primary (or cryopreserved) human hepatocytes (PHs). We recently demonstrated that stage-specific transient transduction of transcription factors, in addition to treatment with optimal growth factors and cytokines, is useful for promoting hepatic differentiation [3–6]. The hepatocyte-like cells, which have many hepatocyte characteristics (the abilities to uptake low-density lipoprotein and Indocyanine green, store glycogen, and synthesize urea) and drug metabolism capacity, were generated from hESCs/hiPSCs by combinational transduction of FOXA2 and HNF1α [6]. However, further maturation of the hepatocyte-like cells is required because their hepatic characteristics, such as drug metabolism capacity, are lower than those of PHs [6].

To promote further maturation of the hepatocyte-like cells, we subjected them to three-dimensional (3D) spheroid cultures. It is known that various 3D culture conditions (such as Algimatrix scaffolds [7], cell sheet technology [8], galactose-carrying substrata [9], and basement membrane substratum [10]) are useful for the maturation of the hepatocyte-like cells. Nanopillar Plate technology [11] used in the present study makes it easy to control the configuration of the spheroids. The Nanopillar Plate has an arrayed µm-scale hole structure at the bottom of each well, and nanopillars were aligned further at the bottom of the respective holes. The seeded cells evenly drop into the holes, then migrate and aggregate on top surface of the nanopillars, thus likely to form the uniform spheroids in each hole. Not only 3D spheroid cultures [12] but also Matrigel overlay cultures [13] are useful for maintaining the hepatocyte characteristics of PHs. Therefore, we employed both 3D

* Corresponding author. Laboratory of Biochemistry and Molecular Biology, Graduate School of Pharmaceutical Sciences, Osaka University, 1-6 Yamadaoka, Suita, Osaka 565-0871, Japan. Tel.: +81 6 6879 8185; fax: +81 6 6879 8186.
E-mail address: mizuguch@phs.osaka-u.ac.jp (H. Mizuguchi).

0142-9612/$ – see front matter © 2012 Elsevier Ltd. All rights reserved.
http://dx.doi.org/10.1016/j.biomaterials.2012.11.029

spheroid culture and Matrigel overlay culture systems to promote hepatocyte maturation of the hepatocyte-like cells.

The hepatocyte-like cells generated from hESCs/hiPSCs are expected to be used in drug development. To the best of our knowledge, however, few studies have tried to predict widespread drug-induced cytotoxicity *in vitro* using the hepatocyte-like cells. To precisely determine the applicability of the hepatocyte-like cells to drug screening, it is necessary to investigate the responses of these hepatocyte-like cells to many kinds of hepatotoxic drugs.

In this study, 3D spheroid and Matrigel overlay cultures of the hepatocyte-like cells were performed to promote hepatocyte maturation. The gene expression analysis of cytochrome P450 (CYP) enzymes, conjugating enzymes, hepatic transporters, and hepatic nuclear receptors in the 3D spheroid-cultured hESC- or hiPSC-derived hepatocyte-like cells (3D ES-hepa or 3D iPS-hepa), were analyzed. In addition, CYP induction potency and drug metabolism capacity were estimated in the 3D ES/iPS-hepa. To determine the suitability of these cells for drug screening, we examined whether the drug-induced cytotoxicity is induced by treatment of various kinds of hepatotoxic drugs in 3D ES/iPS-hepa.

2. Materials and methods

2.1. hESCs and hiPSCs culture

A hESC line, H1 and H9 (WiCell Research Institute), was maintained on a feeder layer of mitomycin C-treated mouse embryonic fibroblasts (Millipore) with Repro Stem medium (Repro CELL) supplemented with 5 ng/ml fibroblast growth factor 2 (FGF2) (Sigma). Both H1 and H9 were used following the Guidelines for Derivation and Utilization of Human Embryonic Stem Cells of the Ministry of Education, Culture, Sports, Science and Technology of Japan and furthermore, and the study was approved by Independent Ethics Committee.

Three human iPSC lines were provided from the JCRB Cell Bank (Tic, JCRB Number: JCRB1331; Dotcom, JCRB Number: JCRB1327; Toe, JCRB Number: JCRB1338) [14,15]. These human iPSC lines were maintained on a feeder layer of mitomycin C-treated mouse embryonic fibroblasts with iPSellon (Cardio) supplemented with 10 ng/ml FGF2. Other three human iPSC lines, 201B6, 201B7 and 253G1 were kindly provided by Dr. S. Yamanaka (Kyoto University) [2]. These human iPSC lines were maintained on a feeder layer of mitomycin C-treated mouse embryonic fibroblasts with Repro Stem supplemented with 5 ng/ml FGF2.

2.2. In vitro differentiation

Before the initiation of cellular differentiation, the medium of hESCs was exchanged into a defined serum-free medium, hESF9, and cultured as previously reported [16]. The differentiation protocol for the induction of definitive endoderm cells, hepatoblasts, and hepatocytes was based on our previous reports with some modifications [3–5,17]. Briefly, in mesendoderm differentiation, hESCs were dissociated into single cells by using Accutase (Millipore) and cultured for 2 days on Matrigel (BD Biosciences) in differentiation hESF-DIF medium which contains 100 ng/ml Activin A (R&D Systems) and 10 ng/ml bFGF (hESF-DIF medium was purchased from Cell Science & Technology Institute; differentiation hESF-DIF medium was supplemented with 10 μg/ml human recombinant insulin, 5 μg/ml human apotransferrin, 10 μM 2-mercaptoethanol, 10 μM ethanolamine, 10 μM sodium selenite, and 0.5 mg/ml bovine fatty acid free serum albumin [all from sigma]). To generate definitive endoderm cells, the mesendoderm cells were transduced with 3000 vector particle (VP)/cell of Ad-FOXA2 for 1.5 h on day 2 and cultured until day 6 on Matrigel in differentiation hESF-DIF medium supplemented with 100 ng/ml Activin A and 10 ng/ml bFGF. For induction of hepatoblasts, the DE cells were transduced with each 1500 VP/cell of Ad-FOXA2 and Ad-HNF1α for 1.5 h on day 6 and cultured for 3 days on Matrigel in hepatocyte culture medium (HCM) (Lonza) supplemented with 30 ng/ml bone morphogenetic protein 4 (BMP4) (R&D Systems) and 20 ng/ml FGF4 (R&D Systems). In hepatic expansion, the hepatoblasts were transduced with each 1500 VP/cell of Ad-FOXA2 and Ad-HNF1α for 1.5 h on day 9 and cultured for 3 days on Matrigel in HCM supplemented with 10 ng/ml hepatocyte growth factor (HGF), 10 ng/ml FGF1, 10 ng/ml FGF4, and 10 ng/ml FGF10 (all from R&D Systems). To perform hepatocyte maturation on Nanopillar Plate (a prototype multi-well culturing plate for spheroid culture developed and prepared by Hitachi High-Technologies Corporation) shown in Fig. 1B, the cells were seeded at 2.5×10^5 cells/cm^2 (Fig. S1) in hepatocyte culture medium (Fig. S2) supplemented with 10 ng/ml HGF, 10 ng/ml FGF1, 10 ng/ml FGF4, and 10 ng/ml FGF10 on day 11. In the first stage of hepatocyte maturation (from day 12 to day 25), the cells were cultured for 13 days on Matrigel in HCM supplemented with 20 ng/ml HGF, 20 ng/ml oncostatin M (OsM), 10 ng/ml FGF4, and 10^{-6} M dexamethasone (DEX). In the second stage of hepatocyte maturation (from day 25 to day 35), Matrigel was overlaid on the hepatocyte-like cells. Matrigel were diluted to a final concentration of 0.25 mg/ml with William's E medium (Invitrogen) containing 4 mM L-glutamine, 50 ug/ml gentamycin sulfate, 1 × ITS (BD Biosciences), 20 ng/ml OsM, and 10^{-6} M DEX. The culture medium was aspirated, and then the Matrigel solution (described above) was overlaid on the hepatocyte-like cells. The cells were incubated overnight, and the medium was replaced with HCM supplemented with 20 ng/ml OsM and 10^{-6} M DEX.

2.3. Adenovirus (Ad) vectors

Ad vectors were constructed by an improved *in vitro* ligation method [18,19]. The human EF-1α promoter-driven LacZ-, FOXA2-, or HNF1α-expressing Ad vectors (Ad-LacZ, Ad-FOXA2, or Ad-HNF1α, respectively) were constructed previously [3,4,20]. All of Ad vectors contain a stretch of lysine residue (K7) peptides in the C-terminal region of the fiber knob for more efficient transduction of hESCs, hiPSCs, and DE cells, in which transfection efficiency was almost 100%, and purified as described previously [3–5]. The vector particle (VP) titer was determined by using a spectrophotometric method [21].

2.4. Flow cytometry

Single-cell suspensions of hESC/hiPSC-derived cells were fixed with 2% paraformaldehyde (PFA) at 4°C for 20 min, and then incubated with the primary antibody (described in Table S1), followed by the secondary antibody (described in Table S1). Flow cytometry analysis was performed using a FACS LSR Fortessa flow cytometer (BD Biosciences).

2.5. RNA isolation and reverse transcription-polymerase chain reaction (RT-PCR)

Total RNA was isolated from hESCs or hiPSCs and their derivatives using ISOGENE (Nippon Gene). cDNA was synthesized using 500 ng of total RNA with a Superscript VILO cDNA synthesis kit (Invitrogen). Real-time RT-PCR was performed with Taqman gene expression assays (Applied Biosystems) or SYBR Premix Ex Taq (TaKaRa) using an ABI PRISM 7000 Sequence Detector (Applied Biosystems). Relative quantification was performed against a standard curve and the values were normalized against the input determined for the housekeeping gene, glyceraldehyde 3-phosphate dehydrogenase (GAPDH). The primer sequences used in this study are described in Table S2.

2.6. Immunohistochemistry

The cells were fixed with 4% PFA. After incubation with 1% Triton X-100, blocking with Blocking One (Nakalai tesque), the cells were incubated with primary antibody (describe in Table S1) at 4°C for over night, followed by incubation with a secondary antibody (described in Table S1) at room temperature for 1 h.

2.7. ELISA

The hESCs or hiPSCs were differentiated into hepatocytes as described in Fig. 1A. The culture supernatants, which were incubated for 24 h after fresh medium was added, were collected and analyzed for the amount of ALB secretion by ELISA. ELISA kits for ALB were purchased from Bethyl. ELISA was performed according to the manufacturer's instructions. The amount of ALB secretion was calculated according to each standard followed by normalization to the protein content per well.

2.8. Urea secretion

The hESCs or hiPSCs were differentiated into hepatocytes as described in Fig. 1A. The culture supernatants, which were incubated for 24 h after fresh medium was added, were collected and analyzed for the amount of urea secretion. Urea measurement kits were purchased from BioAssay Systems. The experiment was performed according to the manufacturer's instructions. The amount of urea secretion was calculated according to each standard followed by normalization to the protein content per well.

2.9. Canalicular secretory assay

At cellular differentiation, the hepatocyte-like cell spheroids were treated with 5 mM choly-lysyl-fluorescein (CLF) (BD Biosciences) for 30 min. The cells were washed with culture medium, and then observed by fluorescence microscope. To inhibit the function of BSEP, the cells were pretreated with Cyclosporin A 24 h before of the CLF treatment.

2.10. Assay for CYP activity and CYP induction

To measure the cytochrome P450 2C9 and 3A4 activity of the cells, we performed lytic assays by using a P450-GloTM CYP2C9 (catalog number; V8791) and

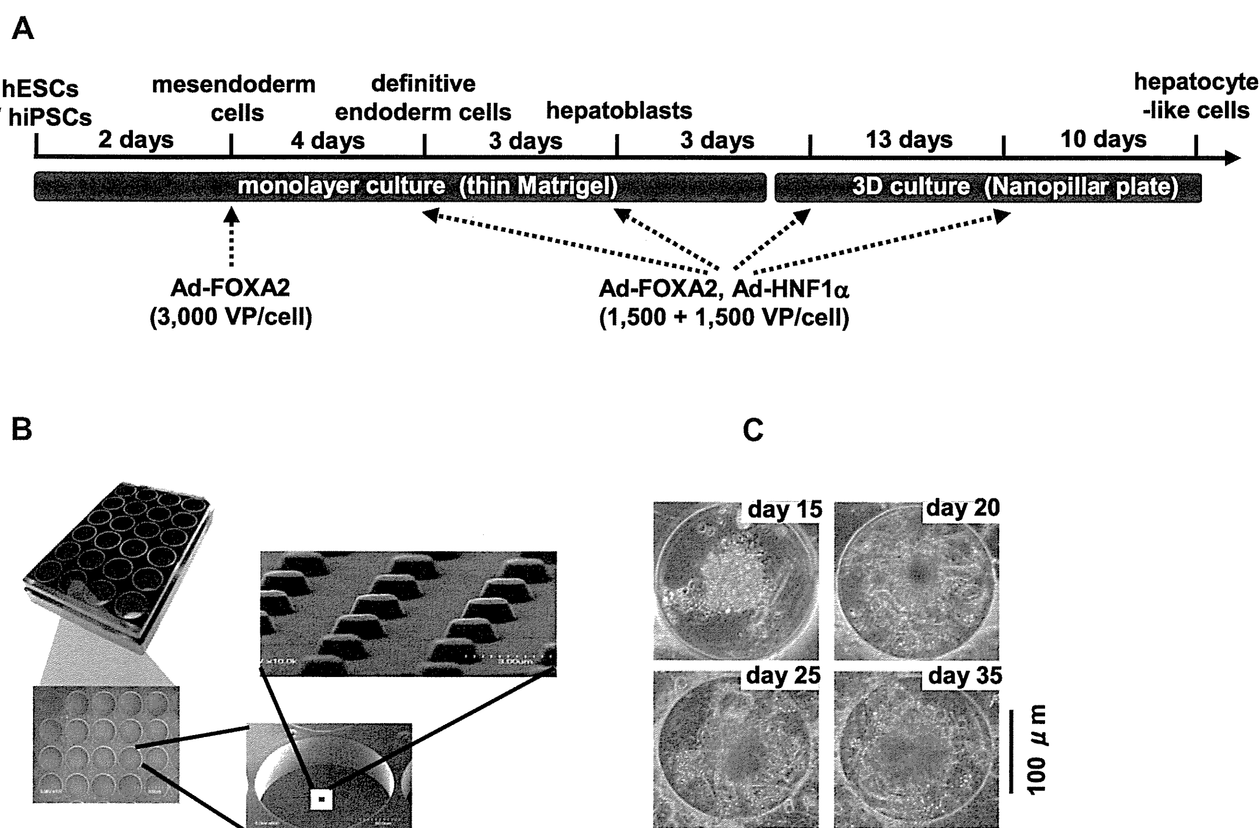

Fig. 1. Hepatocyte-like cells were differentiated from hESCs/hiPSCs by using Nanopillar Plate. (A) The procedure for differentiation of hESCs into 3D ES/iPS-hepa via mesendoderm cells, definitive endoderm cells, and hepatoblasts is presented schematically. In the differentiation, not only the addition of growth factors but also stage-specific transient transduction of both FOXA2- and HNF1α-expressing Ad vector (Ad-FOXA2 and Ad-HNF1α, respectively) was performed. The cellular differentiation procedure is described in detail in the materials and methods section. (B) Photograph display of a 24-well format Nanopillar Plate and its microstructural appearances of the hole and pillar structure. (C) Phase-contrast micrographs of the hESC-hepa spheroids on the Nanopillar Plate are shown. Scale bar represents 100 μm.

3A4 (catalog number; V9001) Assay Kit (Promega), respectively. We measured the fluorescence activity with a luminometer (Lumat LB 9507; Berthold) according to the manufacturer's instructions. The CYP activity was normalized with the protein content per well.

To measure CYP2C9 and 3A4 induction potency, the CYP activity was measured by using a P450-GloTM CYP2C9 and 3A4 Assay Kit, respectively. The cells were treated with rifampicin, which is known to induce both CYP2C9 and 3A4, at a final concentration of 10 μM for 48 h. The cells were also treated with Ketoconazole (Sigma) or Sulfaphenazole (Sigma), which are inhibitors for CYP3A4 or 2C9, at a final concentration of 1 μM or 2 μM, respectively, for 48 h. Controls were treated with DMSO (final concentration 0.1%). Inducer compounds were replaced daily.

2.11. Cell viability tests

Cell viability was assessed by the WST-8 assay kit (Dojindo) in Fig. 2D. After treatment with test compounds, such as Acetaminophen (Wako), Allopurinol (Wako), Amiodaron (Sigma), Benzbromarone (Sigma), Clozapine (Wako), Cyclizine (MP bio), Dantrolene (Wako), Desipramine (Wako), Disufliram (Wako), Erythromycin (Wako), Felbamate (Sigma), Flutamide (Wako), Isoniazid (Sigma), Labetalol (Sigma), Lefunomide (Sigma), Maprotiline (Sigma), Nefazodone (Sigma), Nitrofurantoin (Sigma), Sulindac (Wako), Tacrine (Sigma), Tebinafine (Wako), Tolcapone (TRC), Troglitazone (Wako), and Zafirlukast (Cayman) for 24 h, the cell viability was measured. The cell viability of the 3D iPSC-hepa were assessed by WST-8 assay after 24 h exposure to different concentrations of Aflatoxin B1 (Sigma) and Benzbromarone in the presence or absence of the CYP3A4 or 2C9 inhibitor, Ketoconazole (1 μM) or Sulfaphenazole (10 μM), respectively. The control refers to incubations in the absence of test compounds and was considered as 100% viability value. Controls were treated with DMSO (final concentration 0.1%). ATP assay (BioAssay Systems), Alamar Blue assay (Invitrogen), and Crystal Violet (Wako) staining assay were performed according to the manufacturer's instructions.

2.12. Primary human hepatocytes

Three lots of cryopreserved human hepatocytes (lot Hu8072 [CellzDirect], HC2-14, and HC10-101 [Xenotech]) were used. These three lots of crypreserved human hepatocytes were cultured according to our previous report [5].

2.13. Statistical analysis

Statistical analysis was performed using the unpaired two-tailed Student's *t*-test. All data are represented as means ± SD ($n = 3$).

3. Results

The 3D ES/iPS-hepa were generated from hESCs/hiPSCs as shown in Fig. 1A. Hepatocyte differentiation of hESCs/hiPSCs was efficiently promoted by stage-specific transient transduction of FOXA2 and HNF1α in addition to the treatment with appropriate soluble factors (growth factors and cytokines) [6]. On day 11, the hESC-derived cells were seeded at 2.5×10^5 cells/cm^2 (Fig. S1) on Nanopillar Plate (Fig. 1B), in hepatocyte culture medium (Fig. S2) to promote hepatocyte maturation. In addition, Matrigel was overlaid on the 3D ES-hepa to promote further hepatocyte maturation. The 3D ES-hepa with compact morphology that were adhesive to the substratum and had an optimal size (approximately 100 μm in diameter) were formed by using the Nanopillar Plate (Fig. 1C). The spheroids seem to be stable because they could be cultured for more than 20 days. We have confirmed that more than 90% of the cells that constitute the spheroids were alive, indicating that the necrotic centers are absent.

To investigate whether or not a 3D spheroid culture could promote hepatocyte maturation of the hepatocyte-like cells, various hepatocyte characteristics of the 3D ES/iPS-hepa were compared with those of the monolayer-cultured hESC- or hiPSC-derived hepatocyte-like cells (mono ES-hepa or mono iPS-hepa). The gene expression level of *ALB* peaked on day 20 in the mono ES-hepa, and then it was dramatically decreased after day 25 (Fig. 2A). In contrast, the gene expression level of *ALB* was

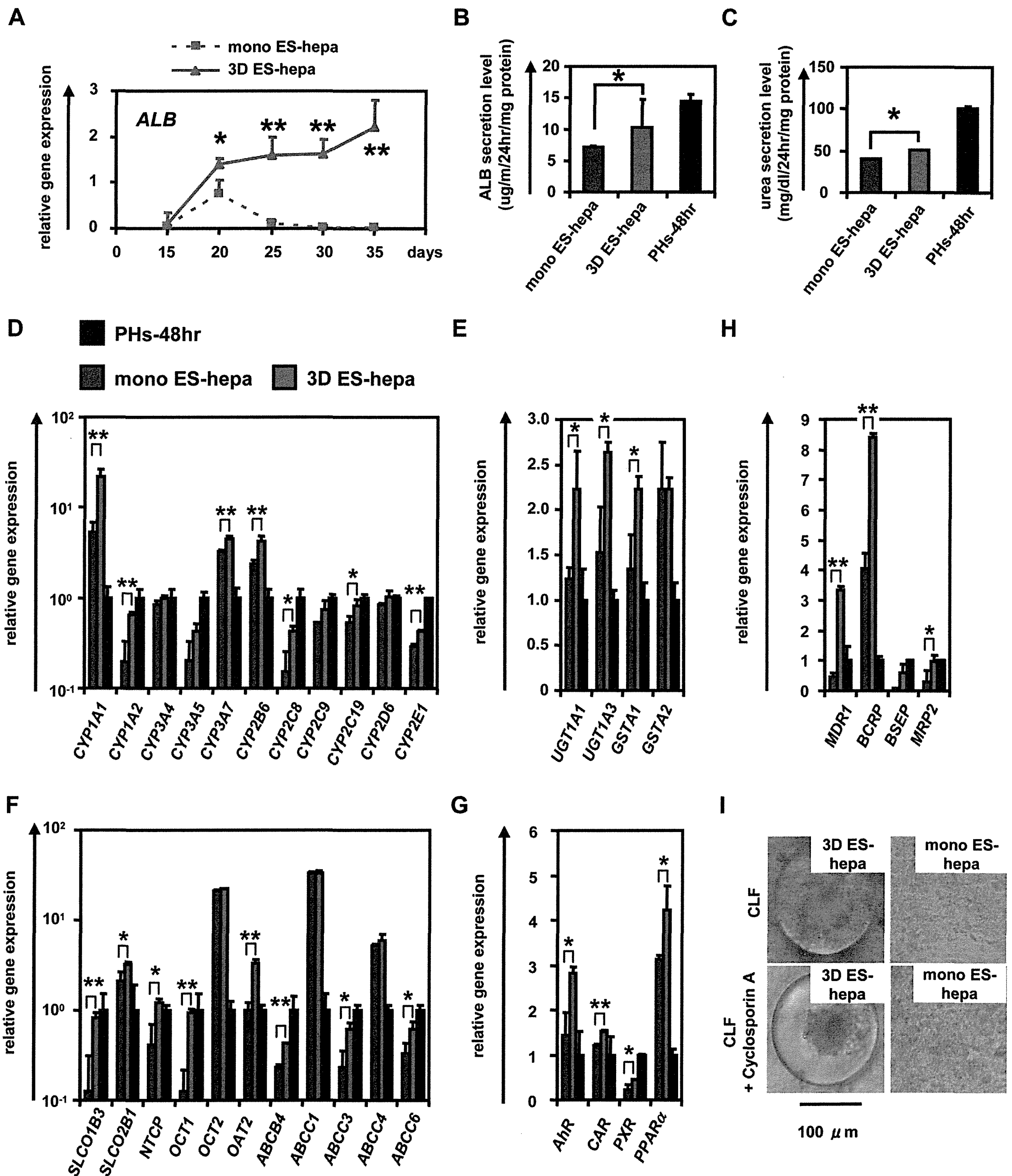

Fig. 2. Hepatocyte functions in hESC-derived hepatocyte-like cells were enhanced by using Nanopillar Plate. (A) The gene expression levels of *ALB* were measured by real-time RT-PCR on day 15, 20, 25, 30, and 35. On the *y* axis, the gene expression levels in PHs (three lots of PHs were used in all studies), which were cultured for 48 h after plating (PHs-48hr), were taken as 1.0. (B, C) The amount of ALB (B) and urea (C) secretion were examined in the mono ES-hepa (day 20), the 3D ES-hepa (day 35), and PHs-48hr. (D–H) The gene expression levels of CYP enzymes (D), conjugating enzymes (E), hepatic transporters (F), hepatic nuclear receptors (G), and bile canaliculi transporters (H) were examined by real-time RT-PCR in the mono ES-hepa, the 3D ES-hepa, and PHs-48hr. On the *y* axis, the expression levels in PHs-48hr were taken as 1.0. (I) The ability of bile acid uptake and efflux was examined in the mono ES-hepa and 3D ES-hepa. Choly-lysyl-fluorescein (CLF) (5 μM) was used for the observation of bile canaliculi uptake and efflux. To inhibit transportation by BSEP, the cells were pretreated with 1 μM Cyclosporin A. $^{*}P < 0.05$; $^{**}P < 0.01$.

moderately increased in the 3D ES-hepa until day 35 (Fig. 2A). These results suggest that the hepatocyte functions of the 3D ES-hepa are sustained for more than 2 weeks on the Nanopillar Plate, although those of the mono ES-hepa are rapidly devitalized (Fig. 2A and Fig. S4). Other hepatocyte characteristics, such as ability of ALB and urea secretion and gene expression levels of hepatocyte-related markers in the 3D ES-hepa were compared with those of the mono ES-hepa (Fig. 2B–H). Because the gene expression level of *ALB* in the 3D ES-hepa was the highest on day 35 and that in mono ES-hepa was the highest on day 20, various hepatocyte characteristics were compared on day 35 or day 20, respectively. The amount of ALB (Fig. 2B) and urea (Fig. 2C) secretion in the 3D ES-hepa was higher than those of the mono ES-hepa. The gene expression levels of CYP enzymes (Fig. 2D), conjugating enzymes (Fig. 2E), hepatic transporters (Fig. 2F), hepatic nuclear receptors (Fig. 2G), and hepatic transcription factors (Fig. S5) in the 3D ES-hepa were higher than those in the mono ES-hepa. The expression levels of most of the genes in the 3D ES-hepa were higher than those in the mono ES-hepa. Because the previous study [11] showed that hepatocyte spheroids expressed hepatocyte transporters similar to those of the bile canaliculi in native liver tissue, the gene expression levels of bile canaliculi transporters (Fig. 2H), as well as the ability of bile acid uptake and efflux, (Fig. 2I) were examined in the 3D ES-hepa. The gene expression levels of bile canaliculi transporters were increased in the 3D ES-hepa compared with those of mono ES-hepa and PHs (Fig. 2H). The bile canaliculi formation was visualized by BSEP fluorescent substrate: Cholyl-lysyl-fluorescein (CLF), which is inhibited by BSEP

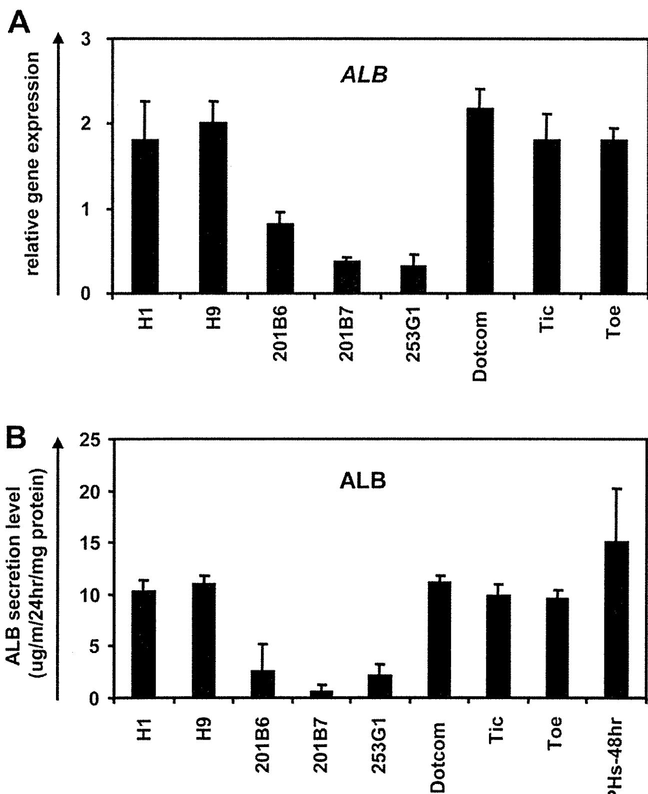

Fig. 3. Comparison of the hepatic differentiation capacities of various hESC and hiPSC lines hESCs (H1 and H9) and hiPSCs (201B6, 201B7, 253G1, Dotcom, Tic, and Toe) were differentiated into the 3D ES/iPS-hepa as described in Fig. 1A. (A) On day 20, the gene expression level of *ALB* was examined by real-time RT-PCR. On the y axis, the gene expression level of *ALB* in PHs-48hr was taken as 1.0. (B) On day 20, the amount of ALB secretion was examined by ELISA. The amount of ALB secretion was calculated according to each standard followed by normalization to the protein content per well.

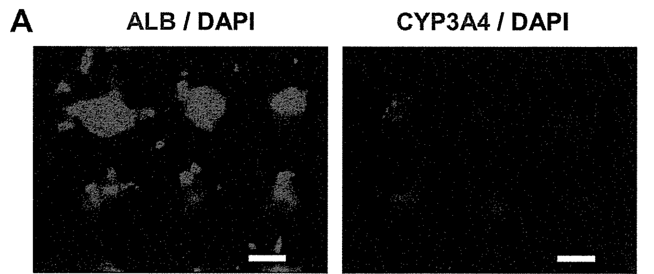

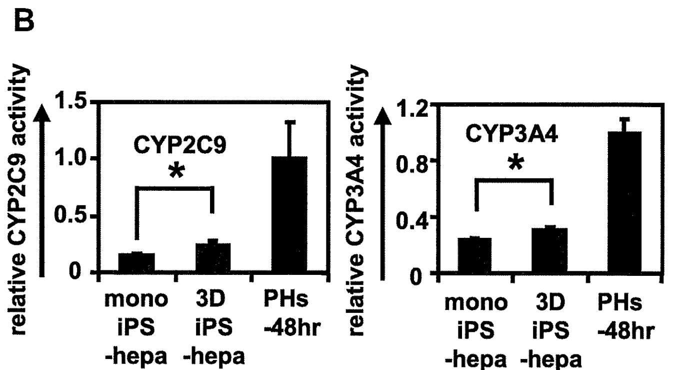

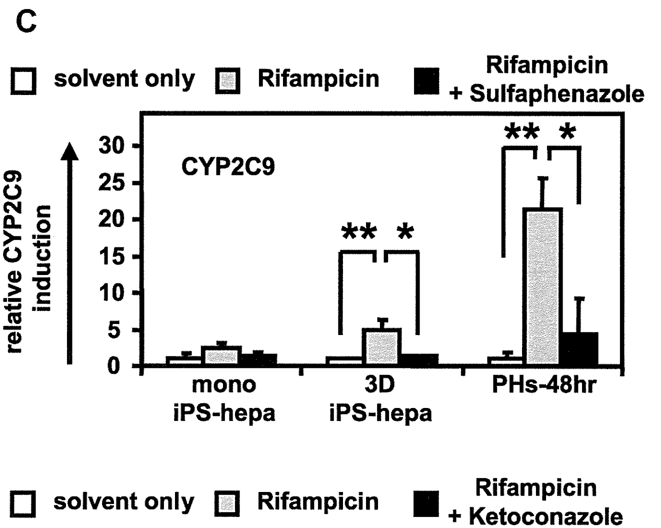

Fig. 4. Drug metabolism capacity and CYP induction potency were examined in the 3D iPS-hepa. (A) The 3D iPS-hepa (day 35) were subjected to immunostaining with anti-ALB (green) or CYP3A4 (red) antibodies. Nuclei were counterstained with DAPI (blue). Scale bar represents 100 μm. (B) The CYP activity was measured in the mono iPS-hepa (day 20), the 3D iPS-hepa (day 35), and PHs-48hr. On the y axis, the CYP activity in PHs-48hr was taken as 1.0. (C) Induction of CYP2C9 (left) or CYP3A4 (right) by DMSO (solvent only; white bar), Rifampicin (gray bar), or rifampicin and CYP inhibitor (Sulfaphenazole or Ketoconazole, black bar) in the mono iPS-hepa, the 3D iPS-hepa, and PHs-48hr. On the y axis, the CYP activity of the cells that have been cultured in DMSO-containing medium was taken as 1.0. *$P < 0.05$; **$P < 0.01$.

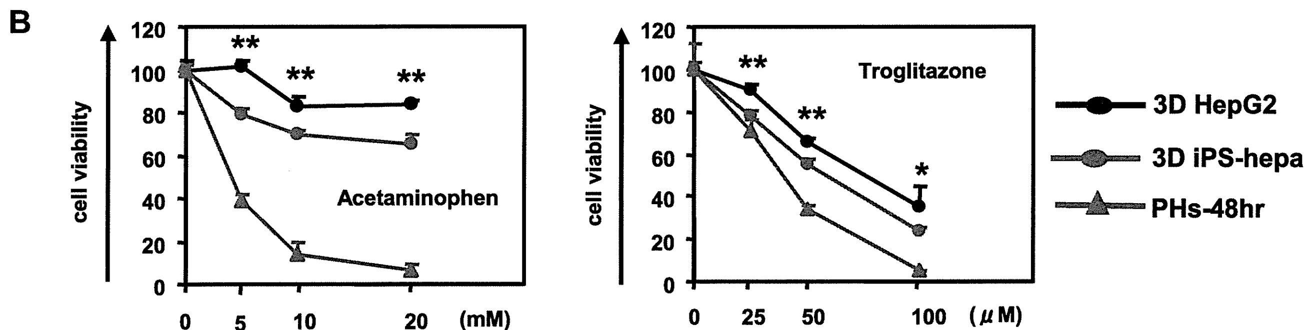
A
3D HepG2
3D iPS-hepa
Allopurinol
Amiodaron
Benzbromarone
Clozapine
Cyclizine
Dantrolene
Desipramine
Disufliram
Erythromycin
Felbamate
Flutamide
Isoniazid
Labetalol
Leflunomide
Maprotiline
Nefazodone
Nitrofurantoin
Sulindac
Tacrine
Tebinafine
Tolcapone
Zafirlukast
cell viability
(μM)
B
Acetaminophen
(mM)
Troglitazone
cell viability
3D HepG2
3D iPS-hepa
PHs-48hr

inhibitor Cyclosporin A [22,23]. More CLF was accumulated in the 3D ES-hepa than in the mono ES-hepa (Fig. 2I *upper panel*). Moreover, CLF accumulation was inhibited by Cyclosporin A treatment only in the 3D ES-hepa (Fig. 2I *lower panel*), demonstrating that the functionality of BSEP transporter in 3D ES-hepa was greater than that in mono ES-hepa. These results suggested that hepatocyte maturation was promoted by the culture on the Nanopillar Plate. It is likely that, compared to the monolayer culture condition, the 3D spheroid-culture condition is more similar to the *in vivo* condition.

It is important to select an hESC/hiPSC line that has a strong ability to differentiate into hepatocyte-like cells in the case of medical applications such as drug screening. In this study, two hESC lines and six hiPSC lines were differentiated into the hepatocyte-like cells, and then their gene expression levels of *ALB* (Fig. 3A) and ALB secretion levels (Fig. 3B) were compared. These results suggest that the iPSC line, Dotcom, was the suitable cell line for hepatocyte maturation. Therefore, the iPSC line, Dotcom, was used to examine the possibility of the 3D iPS-hepa for drug screening. The drug metabolism capacity and the CYP induction potency of the 3D iPS-hepa were compared with those of the mono iPS-hepa. We confirmed the expression of ALB and CYP3A4 protein in the 3D ES-hepa (Fig. 4A). The activity levels of CYP enzymes in the 3D iPS-hepa were measured according to the metabolism of the CYP2C9 or CYP3A4 substrates (Fig. 4B); the levels were higher than those of the mono iPS-hepa (Fig. 4B). We further tested the induction of CYP2C9 and CYP3A4 by chemical stimulation (rifampicin was used as a CYP2C9 or CYP3A4 inducer). Compared with mono iPS-hepa, the 3D iPS-hepa produced more metabolites in response to chemical stimulation (Fig. 4C). In addition, the CYP induction was inhibited by using CYP2C9 or CYP3A4 inhibitor (Sulfaphenazole or Ketoconazole, respectively). These results indicated that drug metabolism capacity and CYP induction potency in 3D iPS-hepa were higher than those in mono iPS-hepa.

Many researchers have tried to predict the drug-induced cytotoxicity *in vitro* using hepatocarcinoma-derived cells such as HepG2 cells [24,25]. HepG2 cells are less expensive than PHs and the reproducible experiments are easier to perform than they are with PHs, although 30% of the compounds were incorrectly classified as nontoxic [24,25]. To overcome these problems, hESC/hiPSC-derived hepatocyte-like cells are expected to be used to predict drug-induced cytotoxicity. To examine its applicability to drug screening, the 3D iPS-hepa were treated with various drugs, that cause hepatotoxicity. WST-8 assay was performed to evaluate cell viability (Fig. S6). The susceptibility of the 3D iPS-hepa to most of the hepatotoxic drugs was higher than that of the mono iPS-hepa (Fig. S7). Compared to the mono iPS-hepa, the 3D iPS-hepa were more suitable tools for drug screening. Next, the susceptibility of the 3D iPS-hepa to the hepatotoxic drugs was compared with that of the 3D spheroid cultured HepG2 cells (3D HepG2; the hepatocyte functions of 3D HepG2 cells are higher than those of monolayer cultured HepG2 cells [Fig. S8]). With most of the drugs, the cell viability of the 3D iPS-hepa was lower than that of the 3D HepG2 (Fig. 5A). These results indicated that the 3D iPS-hepa are more valuable tools for drug screening than the 3D HepG2. However, the susceptibility of the 3D iPS-hepa to Acetaminophen and Troglitazone was lower than that of the PHs which were cultured for 48 h after the cells were plated (Fig. 5B). These results might be due to the lower activity levels of CYPs in 3D iPS-hepa as compared as those in PHs. Taken together, 3D iPS-hepa are more valuable tools for drug screening than the 3D HepG2, although further maturation of 3D iPS-hepa is still required for 3D iPS-hepa to be an alternative cell source of PHs in the drug screening.

To examine whether drug-induced cytotoxicity is caused by CYP metabolites in 3D iPS-hepa, Aflatoxin B1 (mainly metabolized by CYP3A4 [26]) and Benzbromarone (mainly metabolized by CYP2C9 [27]) were treated in the presence or absence of a CYP3A4 and a 2C9 inhibitor, Ketoconazole and Sulfaphenazole, respectively (Fig. 6). The cell viability of 3D iPS-hepa was partially rescued by treatment with the CYP inhibitor. These results indicated that drug-induced cytotoxicity was caused by CYP metabolites of Aflatoxin B1 and Benzbromarone.

4. Discussion

Recently, it has been expected that human pluripotent stem cells and their derivatives, including hepatocyte-like cells, will be utilized in applications for the safety assessment of drugs. We have previously reported that combinational overexpression of SOX17, HEX, and HNF4α, or combinational overexpression of FOXA2 and HNF1α could promote hepatocyte differentiation [5,6]. However, the drug metabolism capacity of the hepatocyte-like cells generated by our previous protocol was still lower than that of primary human hepatocytes [6]. To generate more matured hepatocyte-like cells as compared with our previous protocol, we established a hepatocyte differentiation method employing not only stage-specific transient overexpression of hepatocyte-related transcription factors but also a 3D culture systems using a Nanopillar Plate, was established. Although the use of hepatocyte-like cells generated from hESCs/hiPSCs in application for drug toxicity testing has begun to be focused, to the best of our knowledge, there have been few studies that have investigated whether hepatocyte-like cells could predict many kinds of drug-induced toxicity.

3D culture spheroids were generated from hESCs/hiPSCs by using a Nanopillar Plate. The diameter of the spheroids was approximately 100 μm on day 35 of differentiation (Fig. 1C). Because it is known that the no-oxygen limitation would take place in spheroids up to 100 μm in diameter [28], the size of the spheroid might be important to generate spheroids with high viability. A Nanopillar Plate has a potential to regulate the spheroid diameter simply by culturing under optimized seeding condition, on its suitably designed pillar and hole structure [11]. Therefore, a Nanopillar Plate would be a suitable environment for the generation of 3D ES/iPS-hepa that show high viability and possess high level of hepatocellular functions.

The levels of many hepatocyte functions, such as ALB secretion ability (Fig. 2B), urea secretion ability (Fig. 2C), hepatocyte-related gene expressions (Fig. 2D–H), drug metabolism capacity (Fig. 4B), and CYP induction potency (Fig. 4C), of 3D ES/iPS-hepa were higher than those of mono ES/iPS-hepa. This might have been because the structural and functional polarity, which can be seen in the naïve environment of hepatocytes, of the hepatocyte-like cells was configured by a 3D culturing condition. Previous studies have shown that a 3D culture condition is suitable to maintain the hepatic characteristics of the isolated hepatocytes because this condition mimic *in vivo* environment [29,30]. These facts indicated that the 3D culture condition is a more suitable condition for the hepatocyte-like cells than the monolayer culture condition.

Two hES cell lines and six hiPS cell lines were differentiated into the hepatocyte-like cells in this study. The hiPS cell line, Dotcom, seemed to be a suitable cell line for hepatic differentiation (Fig. 3). Because the hepatic differentiation propensity differs among the

Fig. 5. The possibility of applying 3D iPS-hepa to drug testing was examined. (A) The cell viability of the 3D HepG2 (black) and 3D iPSC-hepa (red) were assessed by WST-8 assay after 24 h exposure to different concentrations of 22 test compounds. (B) The cell viability of the 3D HepG2 (black), 3D iPSC-hepa (red), and PHs-48hr (green) were assessed by WST-8 assay after 24 h exposure to different concentrations of Acetaminophen and Troglitazone. Cell viability is expressed as a percentage of cells treated with solvent only. *$P < 0.05$; **$P < 0.01$.

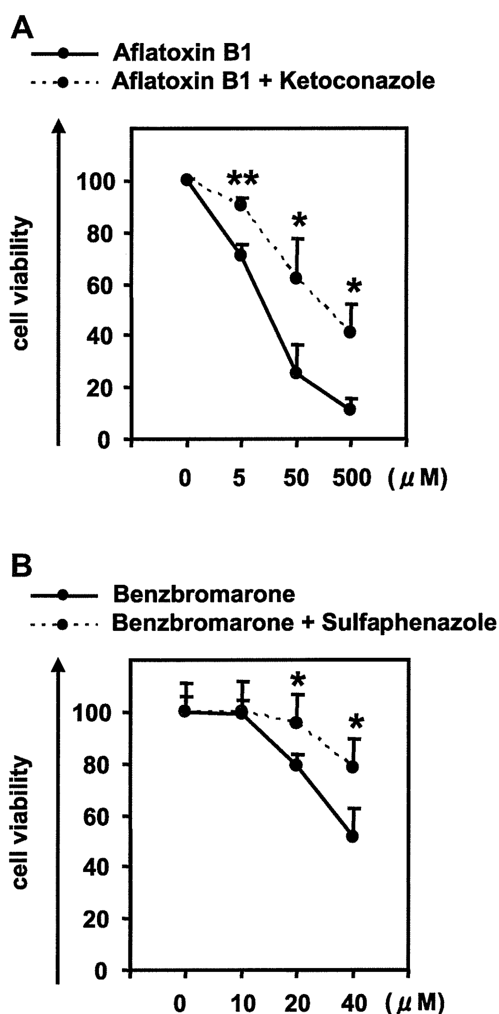

Fig. 6. Drug-induced cytotoxicity in the 3D iPS-hepa is mediated by cytochrome P450. (A, B) The cell viability of the 3D iPSC-hepa was assessed by WST-8 assay after 24 h exposure to different concentrations of (A) Aflatoxin B1 and (B) Benzbromarone in the presence or absence of the CYP3A4 or 2C9 inhibitor, Ketoconazole or Sulfaphenazole, respectively. Cell viability was expressed as the percentage of cells treated with solvent only. $^{*}P < 0.05$; $^{**}P < 0.01$.

hES/hiPS cell lines, it would be important to select an appropriate cell line for medical applications such as drug screening. However, the dominant reason for this hepatic differentiation propensity is not been well known. It would be interesting study to elucidate the mechanism of this propensity.

Although the drug metabolism capacity and CYP induction potency of 3D iPS-hepa were higher than those of mono iPS-hepa (Fig. 4B and C), they were still lower than those of primary human hepatocytes. The hepatic nuclear factors are known to be key molecules in the CYP induction of hepatocytes [30]. Therefore, overexpression of hepatic nuclear factors, which are not abundantly expressed in the hepatocyte-like cells (such as *PXR*), might upregulate the CYP induction potency of the hepatocyte-like cells.

3D iPS-hepa were more sensitive for detection of the drug-induced cytotoxicity than HepG2 cells that are widely used to predict hepatotoxicity [31,32] (Fig. 5). In addition, the decrease of cell viability, which was caused by hepatotoxic drugs, of 3D iPS-hepa was partially rescued by treatment with a CYP inhibitor (Fig. 6). These data suggest that the hepatocyte-like cells could detect the toxicity of the reactive metabolites that were generated by drug metabolizing enzymes such as CYP enzymes. Because in many cases, drug-induced hepatotoxicity is caused by the reactive metabolites produced by drug metabolizing enzymes [33], our finding that the hepatocyte-like cells could detect the toxicity of reactive metabolites should be of great potential for toxicological screening. Moreover, it might be possible to predict idiosyncratic liver toxicity by using hepatocyte-like cells generated from hiPSCs that were established from a patient with a rare CYP polymorphism. However, some compounds did not show any cytotoxicity (such as Cyclizine, Felbamate, and Sulindac) (Fig. 5). To apply the hepatocyte-like cells for wide-spread drug screening, generation of the hepatocyte-like cells are required to detect hepatotoxity in more sensitive manner. Previous studies showed that the depletion of conjugating enzymes [32] or knockdown of Nrf2 [34] expression are useful to upregulate the sensitivity to hepatotoxic drugs. Therefore, these approaches would be useful to generate more sensitive hepatocytes to toxic drugs.

5. Conclusions

In this study, we established the efficient hepatocyte differentiation method which employs not only stage-specific transient overexpression of hepatocyte-related transcription factors but also 3D spheroid culture systems by using Nanopillar Plate. To the best of our knowledge, this is the first study in which the hepatocyte-like cells, having enough hepatocyte functions, mediate drug-induced cytotoxicity against many compounds. Our hepatocyte-like cells differentiated from hESCs or hiPSCs have potential to be applied in drug toxicity testing.

Acknowledgments

We thank Misae Nishijima and Hiroko Matsumura for their excellent technical support. HM, KK, MKF, and TH were supported by grants from the Ministry of Health, Labor, and Welfare of Japan. HM was also supported by Japan Research foundation For Clinical Pharmacology, and The Uehara Memorial Foundation. MKF was also supported by Japan Society for the Promotion of Science Grant-in-Aid for Scientific Research. FS was supported by Program for Promotion of Fundamental Studies in Health Sciences of the National Institute of Biomedical Innovation (NIBIO). We thank Hiromu Yamada (NIBIO) for helpful discussion.

Appendix A. Supplementary data

Supplementary data related to this article can be found at http://dx.doi.org/10.1016/j.biomaterials.2012.11.029.

References

[1] Thomson JA, Itskovitz-Eldor J, Shapiro SS, Waknitz MA, Swiergiel JJ, Marshall VS, et al. Embryonic stem cell lines derived from human blastocysts. Science 1998;282:1145–7.
[2] Takahashi K, Tanabe K, Ohnuki M, Narita M, Ichisaka T, Tomoda K, et al. Induction of pluripotent stem cells from adult human fibroblasts by defined factors. Cell 2007;131:861–72.
[3] Inamura M, Kawabata K, Takayama K, Tashiro K, Sakurai F, Katayama K, et al. Efficient generation of hepatoblasts from human ES cells and iPS cells by transient overexpression of homeobox gene HEX. Mol Ther 2011;19:400–7.
[4] Takayama K, Inamura M, Kawabata K, Tashiro K, Katayama K, Sakurai F, et al. Efficient and directive generation of two distinct endoderm lineages from human ESCs and iPSCs by differentiation stage-specific SOX17 transduction. PLoS One 2011;6:e21780.
[5] Takayama K, Inamura M, Kawabata K, Katayama K, Higuchi M, Tashiro K, et al. Efficient generation of functional hepatocytes from human embryonic stem cells and induced pluripotent stem cells by HNF4alpha transduction. Mol Ther 2012;20:127–37.
[6] Takayama K, Inamura M, Kawabata K, Sugawara M, Kikuchi K, Higuchi M, et al. Generation of metabolically functioning hepatocytes from human pluripotent stem cells by FOXA2 and HNF1alpha transduction. J Hepatol 2012;57:628–36.
[7] Ramasamy TS, Yu JS, Selden C, Hodgson H, Cui W. Application of three-dimensional culture conditions to human embryonic stem cell-derived

definitive endoderm cells enhances hepatocyte differentiation and functionality. Tissue Eng Part A. http://dx.doi.org/10.1089/ten.tea.2012.0190. Available from URL: http://www.ncbi.nlm.nih.gov/pubmed/23003670; 2012.
[8] Nagamoto Y, Tashiro K, Takayama K, Ohashi K, Kawabata K, Sakurai F, et al. The promotion of hepatic maturation of human pluripotent stem cells in 3D co-culture using type I collagen and Swiss 3T3 cell sheets. Biomaterials 2012;33:4526–34.
[9] Meng Q, Haque A, Hexig B, Akaike T. The differentiation and isolation of mouse embryonic stem cells toward hepatocytes using galactose-carrying substrata. Biomaterials 2012;33:1414–27.
[10] Shiraki N, Yamazoe T, Qin Z, Ohgomori K, Mochitate K, Kume K, et al. Efficient differentiation of embryonic stem cells into hepatic cells in vitro using a feeder-free basement membrane substratum. PLoS One 2011;6:e24228.
[11] Takahashi R, Sonoda H, Tabata Y, Hisada A. Formation of hepatocyte spheroids with structural polarity and functional bile canaliculi using nanopillar sheets. Tissue Eng Part A 2010;16:1983–95.
[12] Tong JZ, Sarrazin S, Cassio D, Gauthier F, Alvarez F. Application of spheroid culture to human hepatocytes and maintenance of their differentiation. Biol Cell 1994;81:77–81.
[13] Bi YA, Kazolias D, Duignan DB. Use of cryopreserved human hepatocytes in sandwich culture to measure hepatobiliary transport. Drug Metab Dispos 2006;34:1658–65.
[14] Makino H, Toyoda M, Matsumoto K, Saito H, Nishino K, Fukawatase Y, et al. Mesenchymal to embryonic incomplete transition of human cells by chimeric OCT4/3 (POU5F1) with physiological co-activator EWS. Exp Cell Res 2009;315:2727–40.
[15] Nagata S, Toyoda M, Yamaguchi S, Hirano K, Makino H, Nishino K, et al. Efficient reprogramming of human and mouse primary extra-embryonic cells to pluripotent stem cells. Genes Cells 2009;14:1395–404.
[16] Furue MK, Na J, Jackson JP, Okamoto T, Jones M, Baker D, et al. Heparin promotes the growth of human embryonic stem cells in a defined serum-free medium. Proc Natl Acad Sci U S A 2008;105:13409–14.
[17] Kawabata K, Inamura M, Mizuguchi H. Efficient hepatic differentiation from human iPS cells by gene transfer. Methods Mol Biol 2012;826:115–24.
[18] Mizuguchi H, Kay MA. Efficient construction of a recombinant adenovirus vector by an improved in vitro ligation method. Hum Gene Ther 1998;9:2577–83.
[19] Mizuguchi H, Kay MA. A simple method for constructing E1- and E1/E4-deleted recombinant adenoviral vectors. Hum Gene Ther 1999;10:2013–7.
[20] Tashiro K, Kawabata K, Sakurai H, Kurachi S, Sakurai F, Yamanishi K, et al. Efficient adenovirus vector-mediated PPAR gamma gene transfer into mouse embryoid bodies promotes adipocyte differentiation. J Gene Med 2008;10:498–507.
[21] Maizel Jr JV, White DO, Scharff MD. The polypeptides of adenovirus. I. Evidence for multiple protein components in the virion and a comparison of types 2, 7A, and 12. Virology 1968;36:115–25.
[22] Yasumiba S, Tazuma S, Ochi H, Chayama K, Kajiyama G. Cyclosporin A reduces canalicular membrane fluidity and regulates transporter function in rats. Biochem J 2001;354:591–6.
[23] Roman ID, Fernandez-Moreno MD, Fueyo JA, Roma MG, Coleman R. Cyclosporin A induced internalization of the bile salt export pump in isolated rat hepatocyte couplets. Toxicol Sci 2003;71:276–81.
[24] Rodriguez-Antona C, Donato MT, Boobis A, Edwards RJ, Watts PS, Castell JV, et al. Cytochrome P450 expression in human hepatocytes and hepatoma cell lines: molecular mechanisms that determine lower expression in cultured cells. Xenobiotica 2002;32:505–20.
[25] Hewitt NJ, Hewitt P. Phase I and II enzyme characterization of two sources of HepG2 cell lines. Xenobiotica 2004;34:243–56.
[26] Gallagher EP, Kunze KL, Stapleton PL, Eaton DL. The kinetics of aflatoxin B1 oxidation by human cDNA-expressed and human liver microsomal cytochromes P450 1A2 and 3A4. Toxicol Appl Pharmacol 1996;141:595–606.
[27] Lee MH, Graham GG, Williams KM, Day RO. A benefit-risk assessment of benzbromarone in the treatment of gout. Was its withdrawal from the market in the best interest of patients? Drug Saf 2008;31:643–65.
[28] Glicklis R, Merchuk JC, Cohen S. Modeling mass transfer in hepatocyte spheroids via cell viability, spheroid size, and hepatocellular functions. Biotechnol Bioeng 2004;86:672–80.
[29] Kim K, Ohashi K, Utoh R, Kano K, Okano T. Preserved liver-specific functions of hepatocytes in 3D co-culture with endothelial cell sheets. Biomaterials 2012;33:1406–13.
[30] Khetani SR, Bhatia SN. Microscale culture of human liver cells for drug development. Nat Biotechnol 2008;26:120–6.
[31] Iwamura A, Fukami T, Hosomi H, Nakajima M, Yokoi T. CYP2C9-mediated metabolic activation of losartan detected by a highly sensitive cell-based screening assay. Drug Metab Dispos 2011;39:838–46.
[32] Hosomi H, Akai S, Minami K, Yoshikawa Y, Fukami T, Nakajima M, et al. An in vitro drug-induced hepatotoxicity screening system using CYP3A4-expressing and gamma-glutamylcysteine synthetase knockdown cells. Toxicol In Vitro 2010;24:1032–8.
[33] Guengerich FP, MacDonald JS. Applying mechanisms of chemical toxicity to predict drug safety. Chem Res Toxicol 2007;20:344–69.
[34] Hosomi H, Fukami T, Iwamura A, Nakajima M, Yokoi T. Development of a highly sensitive cytotoxicity assay system for CYP3A4-mediated metabolic activation. Drug Metab Dispos 2011;39:1388–95.

J Gastroenterol (2012) 47:195–202
DOI 10.1007/s00535-011-0481-z

ORIGINAL ARTICLE—LIVER, PANCREAS, AND BILIARY TRACT

Geranylgeranylacetone has anti-hepatitis C virus activity via activation of mTOR in human hepatoma cells

Shigeyuki Takeshita · Tatsuki Ichikawa · Naota Taura · Hisamitsu Miyaaki · Toshihisa Matsuzaki · Masashi Otani · Toru Muraoka · Motohisa Akiyama · Satoshi Miuma · Eisuke Ozawa · Masanori Ikeda · Nobuyuki Kato · Hajime Isomoto · Fuminao Takeshima · Kazuhiko Nakao

Received: 27 July 2010 / Accepted: 29 August 2011 / Published online: 25 October 2011
© Springer 2011

Abstract

Background Geranylgeranylacetone (GGA), an isoprenoid compound which includes retinoids, has been used orally as an anti-ulcer drug in Japan. GGA acts as a potent inducer of anti-viral gene expression by stimulating ISGF3 formation in human hepatoma cells. This drug has few side effects and reinforces the effect of IFN when administered in combination with peg-IFN and ribavirin. This study verified the anti-HCV activity of GGA in a replicon system. In addition, mechanisms of anti-HCV activity were examined in the replicon cells.

Methods OR6 cells stably harboring the full-length genotype 1 replicon containing the *Renilla* luciferase gene, ORN/C-5B/KE, were used to examine the influence of the anti-HCV effect of GGA. After treatment, the cells were harvested with Renilla lysis reagent and then subjected to a luciferase assay according to the manufacturer's protocol.

Result The results showed that GGA had anti-HCV activity. GGA induced anti-HCV replicon activity in a time- and dose-dependent manner. GGA did not activate the tyrosine 701 and serine 727 on STAT-1, and did not induce HSP-70 in OR6 cells. The anti-HCV effect depended on the GGA induced mTOR activity, not STAT-1 activity and PKR. An additive effect was observed with a combination of IFN and GGA.

Conclusions GGA has mTOR dependent anti-HCV activity. There is a possibility that the GGA anti-HCV activity can be complimented by IFN. It will be necessary to examine the clinical effectiveness of the combination of GGA and IFN for HCV patients in the future.

Keywords mTOR · STAT-1 · Interferon · HCV · GGA

Abbreviations

IFN	Interferon
HCV	Hepatitis C virus
STAT	Signal transducers and activators of transcription
ISGF-3	IFN-stimulated gene factor 3
ISRE	IFN-stimulated regulatory element
PKR	Double-stranded RNA-dependent protein kinase
Rapa	Rapamycin
PI3-K	Phosphatidylinositol 3-kinase
mTOR	Mammalian target of rapamycin
GGA	Geranylgeranylacetone
siRNA	Small interfering RNA

S. Takeshita · T. Ichikawa (✉) · N. Taura · H. Miyaaki · T. Matsuzaki · M. Otani · T. Muraoka · M. Akiyama · S. Miuma · E. Ozawa · H. Isomoto · F. Takeshima · K. Nakao
Department of Gastroenterology and Hepatology, Graduate School of Biomedical Sciences, Nagasaki University, 1-7-1 Sakamoto, Nagasaki 852-8501, Japan
e-mail: ichikawa@net.nagasaki-u.ac.jp

M. Ikeda · N. Kato
Department of Molecular Biology, Graduate school of Medicine and Dentistry, Okayama University, Okayama, Japan

Introduction

Currently, chronic hepatitis C virus (HCV) infection is the major cause of hepatocellular carcinoma worldwide [1]. Therefore, an anti-HCV strategy is important for prevention of carcinogenesis. The treatment of HCV with a combination of pegylated interferon (IFN) and ribavirin is effective in 80% of HCV genotype 2 or 3 cases, but less than 50% of genotype 1 cases. New anti-HCV agents have been developed to inhibit the life cycle of HCV and are

used in combination with IFN-α to ameliorate the salvage rate of HCV infection [2]. It is necessary to improve the salvage rate of HCV infection by clarifying the efficacy of IFN treatment since IFN-α is the most basic agent for HCV treatment. Any agents that can support IFN activity will improve the therapeutic effect for HCV infected patients.

Geranylgeranylacetone (GGA), an isoprenoid compound, which includes retinoids, has been used orally as an anti-ulcer drug developed in Japan [3]. GGA protects the gastric mucosa from various types of stress without affecting gastric acid secretion [4, 5]. Moreover, GGA suppresses cell growth and induces differentiation or apoptosis in several human leukemia cells [6, 7]. Another isoprenoid compound, 3,7,11,15-tetramethyl-2,4,6,-10,14-hexadecapentaenoic acid, which is designated as an acyclic retinoid because it has the ability to interact with nuclear retinoid receptors [8], causes apoptosis in certain human hepatoma cells [9]. GGA acts as a potent inducer of antiviral gene expression by stimulating the ISGF3 formation in human hepatoma cells [10]. GGA induces the expression of antiviral proteins such as 2′5′-oligoadenylate synthetase (2′5′-OAS) and double-stranded RNA-dependent protein kinase (PKR) in hepatoma cell lines. GGA stimulates 2′5′-OAS and PKR gene expression at the transcriptional level through the formation of interferon-stimulated gene factor 3 (ISGF-3), which regulates the transcription of both genes. GGA induces the expression of signal transducers and activators of transcription 1, 2 (STAT-1, STAT-2) and p48 proteins, components of ISGF3, together with the phosphorylation of STAT1 [10]. However, no anti-HCV activity was observed.

A cell culture HCV replicon system has been developed as a useful tool for the study of HCV replication and mass screening for anti-HCV reagents. OR6 cells stably harboring the full-length genotype 1 replicon containing the *Renilla* luciferase gene, ORN/C-5B/KE [11], were used to examine the influence of the anti-HCV effect of IFN. The luciferase activity in cell lysate of OR6 was correlated with the HCV-RNA concentration, and the IC50 of IFN-α was less than 10 IU/mL [11]. The OR6 system is a useful and sensitive cell culture replicon system.

This study verified the anti-HCV activity of GGA in the OR6 system. In addition, the mechanisms of anti-HCV activity were examined in OR6 cells.

Materials and methods

Reagents

GGA was a generous gift from Eisai Co. (Tokyo, Japan). Recombinant human IFN-α2a was purchased from Nippon Rosche Co. (Tokyo, Japan). Wortmannin, LY294002, Akt inhibitor and rapamycin were purchased from Calbiochem (La Jolla, CA, USA).

HCV replicon system

OR6 cells stably harboring the full-length genotype 1 replicon, ORN/C-5B/KE, were used to examine the influence of the anti-HCV effect of GGA. The cells were cultured in Dulbecco's modified Eagle's medium (Gibco-BRL, Invitrogen) supplemented with 10% fatal bovine serum, penicillin and streptomycin and maintained in the presence of G418 (300 mg/L; Geneticin, Invitrogen). This replicon was derived from the 1B-2 strain (strain HCV-o, genotype 1b), in which the *Renilla* luciferase gene is introduced as a fusion protein with neomycin to facilitate the monitoring of HCV replication.

Reporter gene assay

The OR6 cells were grown in 24-well plates. One day later, the cells were incubated in the absence or presence of varying concentrations of chemical blockers and GGA. After treatment, the cells were harvested with Renilla lysis reagent (Promega, Madison, WI, USA) and luciferase activity in the cells was determined using a luciferase reporter assay system and a TD-20/20 luminometer. The data were expressed as the relative luciferase activity.

Western blotting and antibodies

Western blotting with anti-STAT-1, anti-PKR (Santa Cruz Biotechnology, Santa Cruz, CA, USA), anti-tyrosine-701 phosphorylated STAT-1, anti-serine-727 phosphorylated STAT-1, anti-serine-2448 phosphorylated mTOR, anti-mTOR, anti-threonine-389 phosphorylated p70S6K, anti-p70S6K (Cell Signaling, Beverly, MA, USA) and anti-HSP70 (Stressmarq Biosciences Inc, Victoria, Canada) was performed as described previously [10]. Briefly, OR6 cells were lysed by the addition of a lysis buffer (50 mmol/L Tris–HCl, pH 7.4, 1% Np40, 0.25% sodium deoxycholate, 0.02% sodium azide, 0.1% SDS, 150 mmol/L NaCl, 1 mmol/L EDTA, 1 mmol/L PMSF, 1 mg/mL each of aprotinin, leupeptin and pepstatin, 1 mmol/L sodium *o*-vanadate and 1 mmol/L NaF). The samples were separated by electrophoresis on 8–12% SDS polyacrylamide gels and electrotransferred to nitrocellulose membranes, and then blotted with each antibody. The membranes were incubated with horseradish peroxidase-conjugated anti-rabbit IgG or anti-mouse IgG, and the immunoreactive bands were visualized using the ECL chemiluminescence system (Amersham Life Science, Buckinghamshire, England).

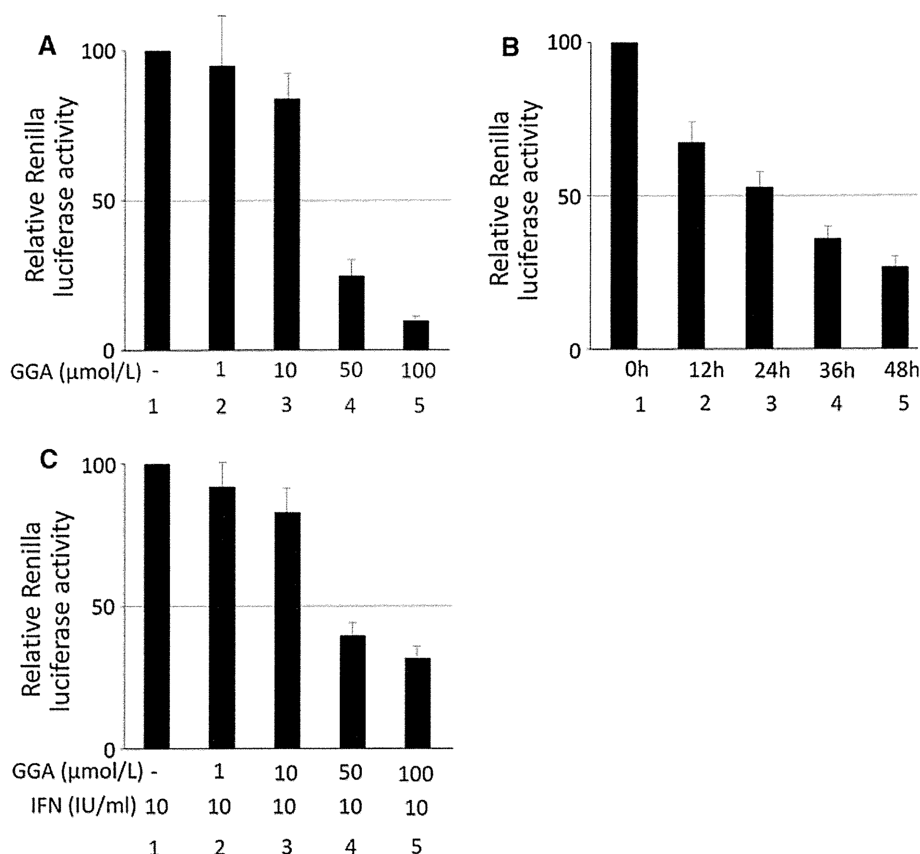

Fig. 1 The effect of GGA on the genome-length HCV RNA replication system. **a** Dose dependent effect of GGA. **b** Time course of GGA suppressed HCV replication. **c** The additive effect of GGA with IFN-α suppressed HCV replication. **a** The OR6 cells were treated with 1–100 μmol/L of GGA (*lanes 2–5*) and *lane 1* was not treated. One day later, *Renilla* luciferase activity was determined by luminometer ($n = 4$). The data are expressed as the mean ± SD and are representative of four similar experiments. The differences between *lane 3* versus *4*, *lane 3* versus *5* and *lane 3* versus *5* were statistically significant. **b** The OR6 cells were treated 50 μmol/L of GGA and at the indicated time, HCV replicon assay was done ($n = 4$). The differences between *lane 1* versus *3–5* and *lane 2* versus *4*, *5* were statistically significant. **c** The OR6 cells were treated with 10 IU/mL of IFN-α in the absence (*lane 1*) or presence of treatment with 1–100 μmol/L of GGA (*lanes 2–5*). Non-treatment OR6 cells has 100% of relative *Renilla* luciferase light unit. The differences between *lane 1* versus *4*, *5* were statistically significant. Statistical significance was accepted as a *P* value of <0.05. The data are expressed as the mean ± SD and are representative of four similar experiments

siRNA transfection assay

mTOR gene knockdown was performed using siRNA (Cell Signaling, Beverly, MA, USA). OR6 cells were transfected with100 nmol/L mTOR specific and non-targeted siRNA as a control in accordance with the appended manual. One day later, the cells were incubated in either the absence or presence of 50 μmol/L GGA.

mTOR kinase activity assay

The cells were washed two times with TBS and lysed by addition of lysis buffer [50 mM Tris HCl, pH 7.4, 100 mM NaCl, 50 mM β-glycerophosphate, 10% glycerol (w/v), 1% Tween-20 detergent (w/v), 1 mM EDTA, 20 nM microcystin-LR, 25 mM NaF, and a cocktail of protease inhibitors]. The insoluble materials were removed by centrifugation at 10,000 rpm for 15 min at 4°C, and the supernatants were collected and subjected to analysis of the mTOR kinase activity using a commercially available kit (Calbiochem, San Diego, USA) according to the manufacturer's instructions.

Results

GGA with or without IFN had anti-HCV activity

OR6 cells, the full-length HCV replication system, were used to examine the effect of GGA. The cells were treated with 1–100 μmol/L of GGA for 24 h and the amount of HCV replicon was measured by the *Renilla* luciferase assay (Fig. 1a). The relative *Renilla* luciferase activity decreased in a dose-dependent manner. Furthermore, GGA